SLAC NATIONAL ACCELERATOR LABORATORY

UCLA

Physics of and Physics with X-ray FELs

C. Pellegrini
UCLA Department of Physics and Astronomy
SLAC National Accelerator Laboratory

2015 Linear Collider School
Whistler, BC, October 27-November 6, 2015

UCLA

Outline

1. Why X-ray lasers?
2. How: high gain free-electron lasers, generating coherent X-ray beams (X-ray FELs).
3. Present status of X-ray FELs.
4. Exploring atomic and molecular science with X-ray FELs.

Outline

UCLA

- The eye and the Sun
- Black body radiation
- Discovery of X-rays
- Invention of lasers
- Atomic transition based lasers; two level model.
- Why X-ray lasers?
- Why X-ray lasers based on atomic transitions are not practical
- Alternative to X-ray lasers: X-ray free-electron lasers (X-ray FELs)
- Radiation from free electrons: Lienard-Wiechert fields, angular and spectral distributions
- Simple oscillating charge
- Undulator radiation properties; helical undulator case.
- Radiation from many electrons
- Simple physical model of the FEL collective instability. 1-D model only, without deriving equations.
- Physical properties of photon sources: Longitudinal and transverse coherence
- Degeneracy number. Examples from various coherent and incoherent sources
- Stimulated radiation
- Basic electron beam requirements for X-ray FELs.
- X-ray FELs development in the USA, Asia and Europe.
- Scientific applications of X-ray FELs. Some examples from physics, chemistry and biology

UCLA

Human eye and observation of natural phenomena

- The homo sapiens' eye, developed during the evolutionary process of our species, is optimized to see in the wavelength region around the green, 0.5 µm, corresponding to the peak intensity of solar radiation. It works like a lens with a diameter d, that of the pupil, about 4 to 5 mm. The angular resolution, determined by light diffraction is $\theta \approx \lambda/d \approx 1/10{,}000$.
- Two points separated by an angle smaller than θ cannot be separated and appear to us as a single point.

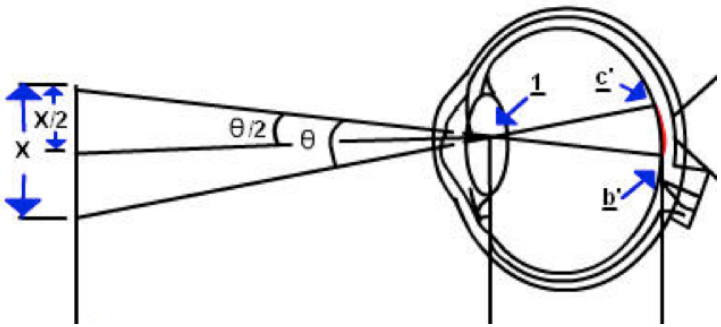

The temporal resolution is about 1/10 s. Changes faster than this appear to us as continuous, as in the case of a movie shot at 30 photograms/s.

Things large and small

UCLA

1. For objects of our daily life, at a distance of about 1m, we can see clearly objects with a size of about 1/10 mm, a human hair.
2. For heavenly bodies, at a distance typical of the solar system, one astronomical unit, 150 millions km, we can resolve points separated by more than 15,000 km, larger than the Earth diameter, 12,000 km. Looking at the Earth from the Sun, or another planet, we could not see the oceans and the mountain chains. In the same way for a terrestrial observer, Mars or Venus appear as a simple light point.

Opacity and transparency for visible light

Visible light is also easily absorbed by most materials. With our human eyes we cannot see inside other bodies or our own bodies.

The Invention of scientific instruments

UCLA

A big step in human evolution too place about 4 centuries ago: the telescope and the microscope gave us a new vision power.

The diameter of the lens of the first telescope used by Galileo was about 4 cm. The resolution increased ten times. We can see details of Venus, like the phases, or the mountains on the Moon.

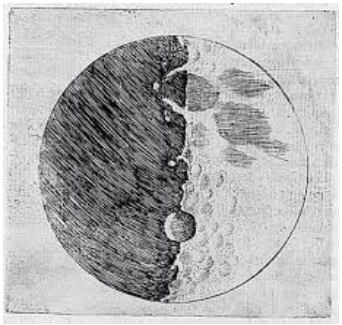

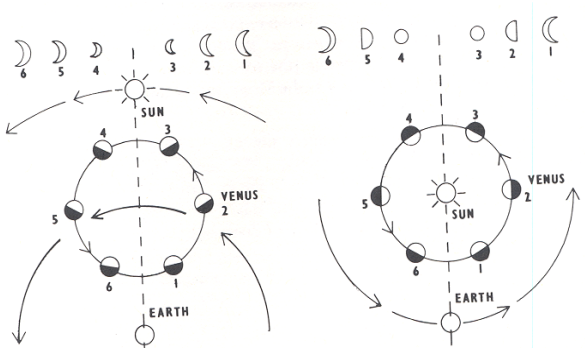

Galileo Galilei, 1610

Galileo's microscope
Resolution: 10 µm 0.1 s.

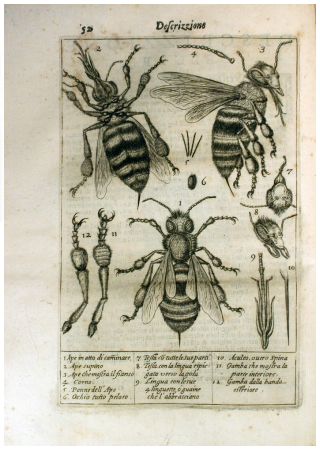

F. Stelluti, 1625

The Starry Messenger (Sidereus Nuncius)

When, for the first time, Galileo looked at the sky with a telescope he saw things never seen before. He writes in the Starry Messenger: "In this short treaties I propose great things for inspection and contemplation by every explorer of Nature. Great, I say, because of the excellence of the things themselves, because of their newness, unheard of through the ages, and also **because of the instrument with the benefit of which they make themselves manifest to our sight**." In that moment humans overcome their biological limits and become Modern Homo Sapiens.

Lens of Galileo's telescope used to make the observations described in the Sidereus Nuncius between 1609 and 1610. Diameter 38mm. Angular resolution is about ten times better than naked eye.

UCLA

The Sun

- The Sun is our main light source. Life on Earth depends on it.
- What are its characteristics?
- The Sun spectrum is that of a source in thermal equilibrium at the temperature T≈6000 K and is given by Planck's law

$$\frac{dU}{dE_{ph}} = \frac{1}{\pi^2 \lambda_C^3} \frac{(E_{ph}/mc^2)^3}{\exp(E_{ph}/k_B T) - 1}$$

$$E_{ph} = \hbar\omega,$$

$$\lambda_C \approx 2.4 \times 10^{-12}\, m,$$

$$k_B \approx 8.6 \times 10^{-5}\, eV/K$$

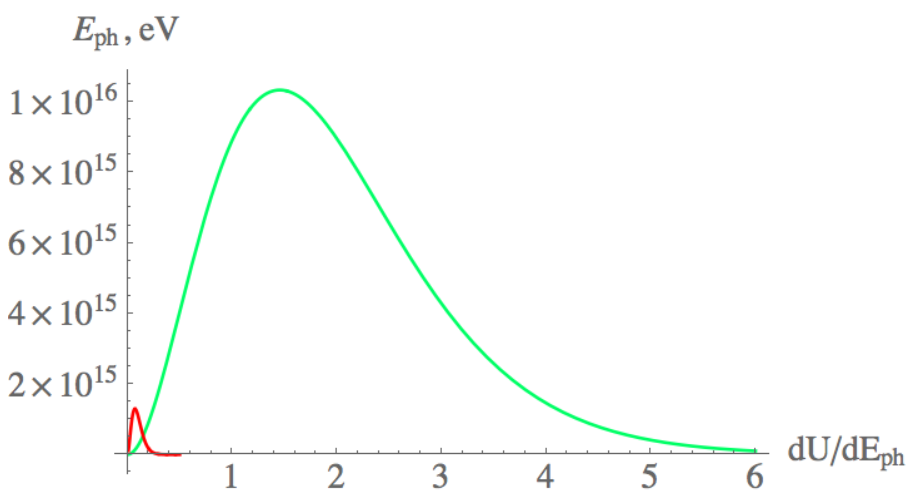

Sun's spectrum, green curve; peaks at about 2eV, ≈0.5μm , green
Black body at human temperature×1000, red curve; peaks at about 0.1eV, ≈ 10μm (IR)

Another kind of light: X-rays

UCLA

On 8 November 1895, Wilhelm Roentgen was working in his lab, studying the properties of a cardboard-shrouded electrical discharge tube, the Crookes tube. He was surprised to see that when the tube was operated, an object across the room began to glow. He called the invisible, mysterious and unknown agent doing it X-rays.

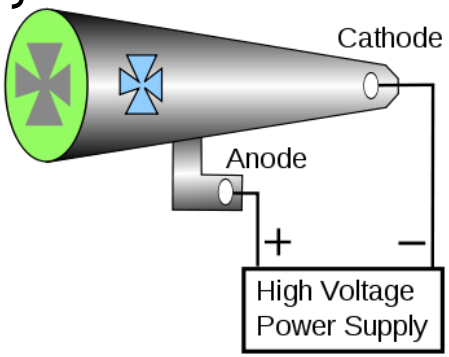

The Crookes tube, a kind of plasma electron accelerator.

In December of the same year he showed that with X-rays we can see inside bodies, a new, very useful, capability.

12/22/1985
Frau
Roentgen's
Hand.

Roentgen won the first Nobel prize in physics in 1901. He did not take any patent on X-rays and their applications.

Invention of the lasers

The lasers were first developed in the 1960s in the infrared.
Following their initial development there was a large interest to develop shorter wavelength lasers, in the visible and UV spectral regions.
The development of an X-Ray lasers, generating coherent, high power, X-ray beams, has been a major goal in laser physics almost from the time the first laser was built in 1960.
A history of laser development can be found in:
Bertolotti, M., 2005, History of the laser, Institute of Physics Publishing, Bristol.
Zinth, W., A. Laubereau and W. Kaiser, 2011, Eur. Physics J. H ***36****, 153.*

Ted Maiman (25 years after first Ruby laser)

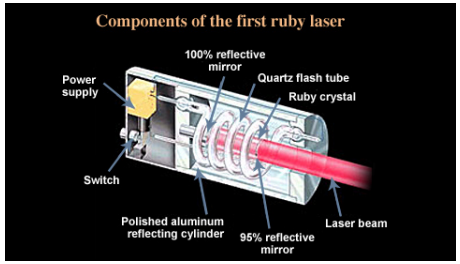

UCLA

Spontaneous and stimulated emission

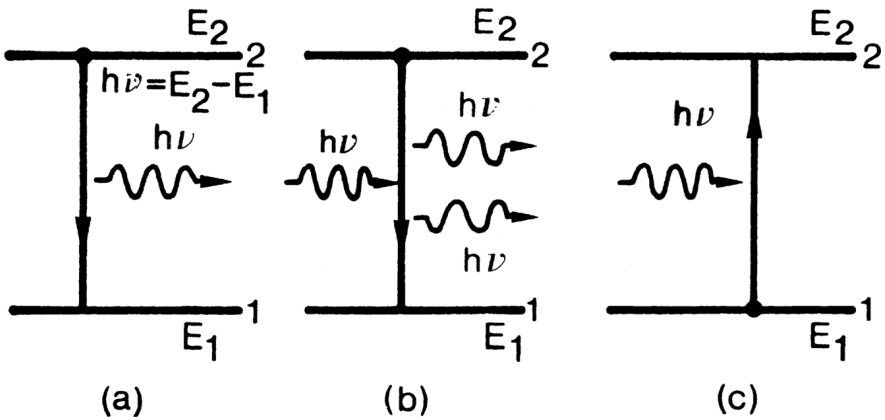

Two levels model. Assume 1 to be the ground state and no degeneracy. Consider only radiative emission.

a. Spontaneous emission: probability for the transition is $\left(dN_2/dt\right)_{sp} = -AN_2$
where A is the Einstein coefficient (rate of radiative decay). 1/A is the radiative lifetime.

b. Stimulated emission: probability for the transition is $\left(dN_2/dt\right)_{st} = -\sigma_{21}FN_2$
where σ_{21} is the stimulated emission cross section, F the photon flux of the incident wave.

c. Stimulated absorption: probability for the transition is $\left(dN_1/dt\right)_{st} = -\sigma_{12}FN_1$
where σ_{12} is the stimulated absorption cross section.

It was shown by Einstein that for non-degenerate levels $\sigma_{21}=\sigma_{12}$.

Laser operation

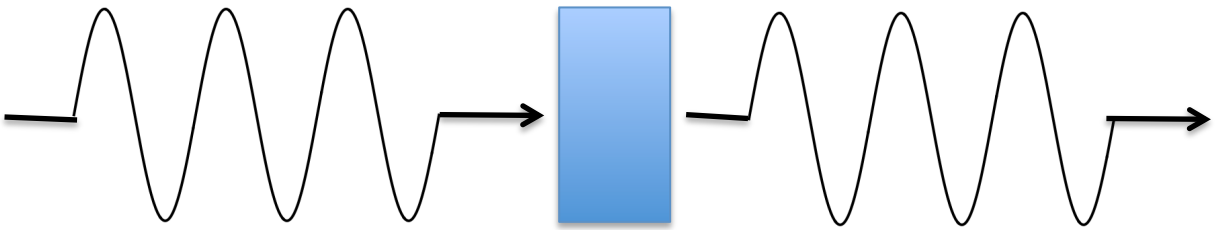

$$dI = \sigma_{21} I \left(N_2 - N_1 \right) dz$$

Amplifier if $N_2 > N_1$, absorber if $N_1 > N_2$.

At thermal equilibrium

$$N_2 / N_1 = e^{-\left(E_2 - E_1\right)/kT}, \; N_2 < N_1$$

Pumping the system we can achieve population inversion, $N_2 > N_1$.
The amount of power needed depends on the energy difference between the two levels and on the radiative lifetime of the excited state that can decay a lower level before population inversion is reached.
Going to shorter wavelengths requires a larger pumping power.

Early work on X-ray lasers

UCLA

The conventional atom-based approach cannot be easily extended to X-rays because of the very short lifetime of excited atom-core quantum energy levels. In addition a larger energy is required to excite electrons in the inner core levels. George Chapline and Lowell Wood (Chapline and Wood,1975) of the Lawrence Livermore National Laboratory estimated the radiative lifetime of an X-ray laser transition would be about 1 fs times the square of the wavelength in angstroms.

Chapline G. and L. Wood,1975, Physics Today ***40****, 8.*

Satisfying these conditions to obtain population inversion requires a very large amount of pumping power. Building low loss optical cavities for X-ray laser oscillators is also difficult, in fact beyond the present state of the art.

Early work on X-ray lasers

Livermore scientists proposed using a nuclear weapon to drive a single pass X-ray laser. They tried the idea in the Dauphin experiment, apparently with success, in 1980. The experiment was part of the Star Wars Defense Initiative: generate an X-ray beam in space, exploding an atomic bomb, to kill incoming missiles. The program was terminated at the end of Star Wars (Hecht 2008).

The development of high peak power, short pulse, visible light lasers made possible another approach: pumping cylindrical plasmas, in some cases also confining the plasma with magnetic fields. These experiments led to X-ray lasing around 18 nm with gain of about 100 in1985 (Matthews *et al*., 1985; Suckewer *et al*., 1985). More work has been done from that time and lasing has been demonstrated at several wavelengths in the soft X-ray region, however with limited peak power and tunability. A review of the most recent work and developments with this approach is given in (Suckewer and Jaeglé, 2009)

Hecht J., 2008, The History of the X-ray Laser, Optics and Photonics News, 19 (2008);
*Matthews D.L. et al., 1985, Physics Review Letters **54**, 110.*
*Suckewer S. et al., 1985, Physics Review Letters **55**, 1753.*
*Suckewer S. and P. Jaeglé, 2009, Laser Physics Letters **1**, 411 (2009).*

UCLA

An alternative solution

The way out of this difficult situation is offered by the generation of electromagnetic waves from relativistic electron beams and the FEL.

A history of this development is found in *Pellegrini, C., 2012, History of the X-ray free-electron laser, European Physics Journal H 37, 659.*

60 cm long undulator used for the first UCLA SASE FEL at 16 µm. Period 1.5 cm, K=1, gap 5mm.
Varfolomeev, A.A., Pellegrini, C., et al., 1992, Large-field-strength short-period undulator design, Nucl. Instr. and Meth. A ***318****, 813.*

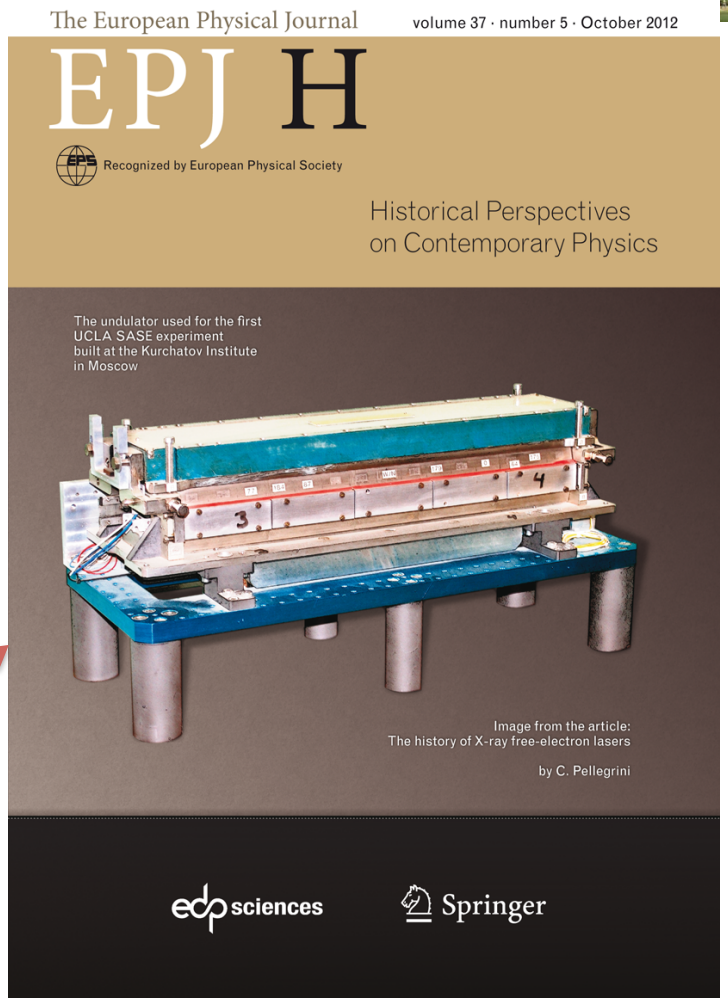

Why x-ray lasers?

A laser generating high intensity, coherent X-ray pulses at Ångstrom wavelength and femtosecond pulse duration -the characteristics time and space scale for atomic and molecular phenomena- allows imaging of periodic and non periodic systems, non crystalline states, studies of dynamical processes in systems far from equilibrium, nonlinear science, opening a new window on atomic and molecular phenomena of interest to biology, chemistry and physics.

UCLA

X-Rays have opened the Ultra-Small World
X-FELs open the Ultra-Small and Ultra-Fast Worlds

Ultra-Small

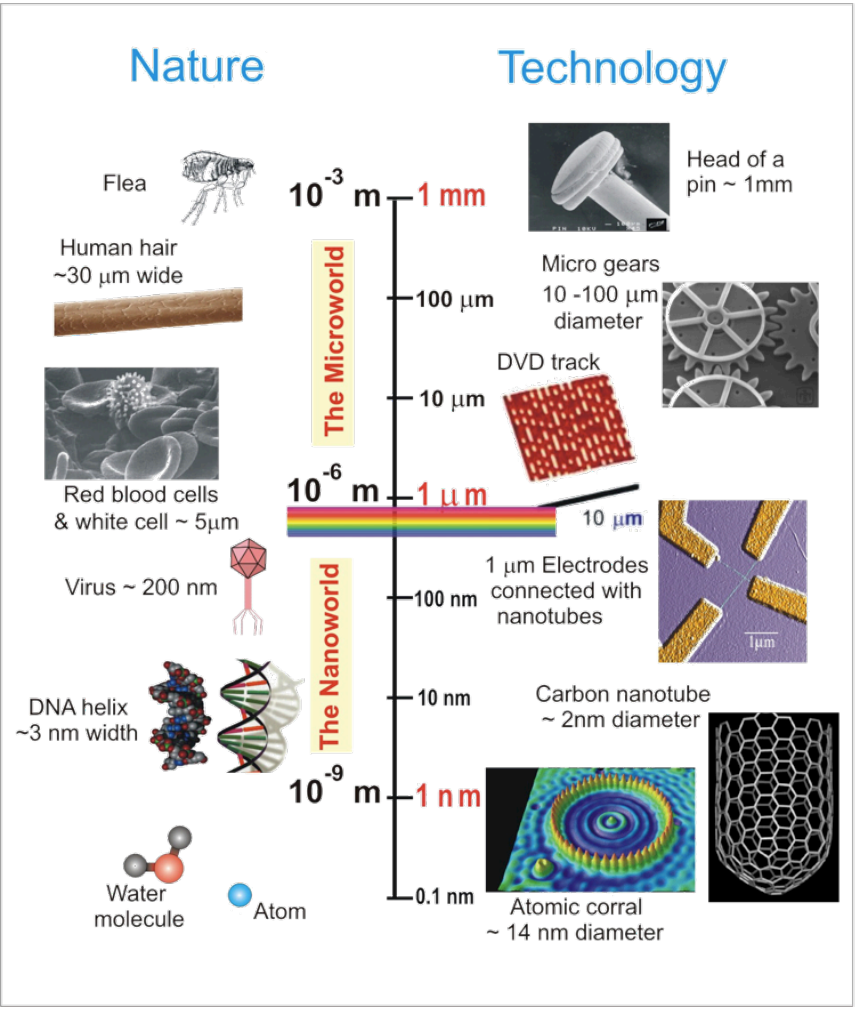

Ultra-Fast

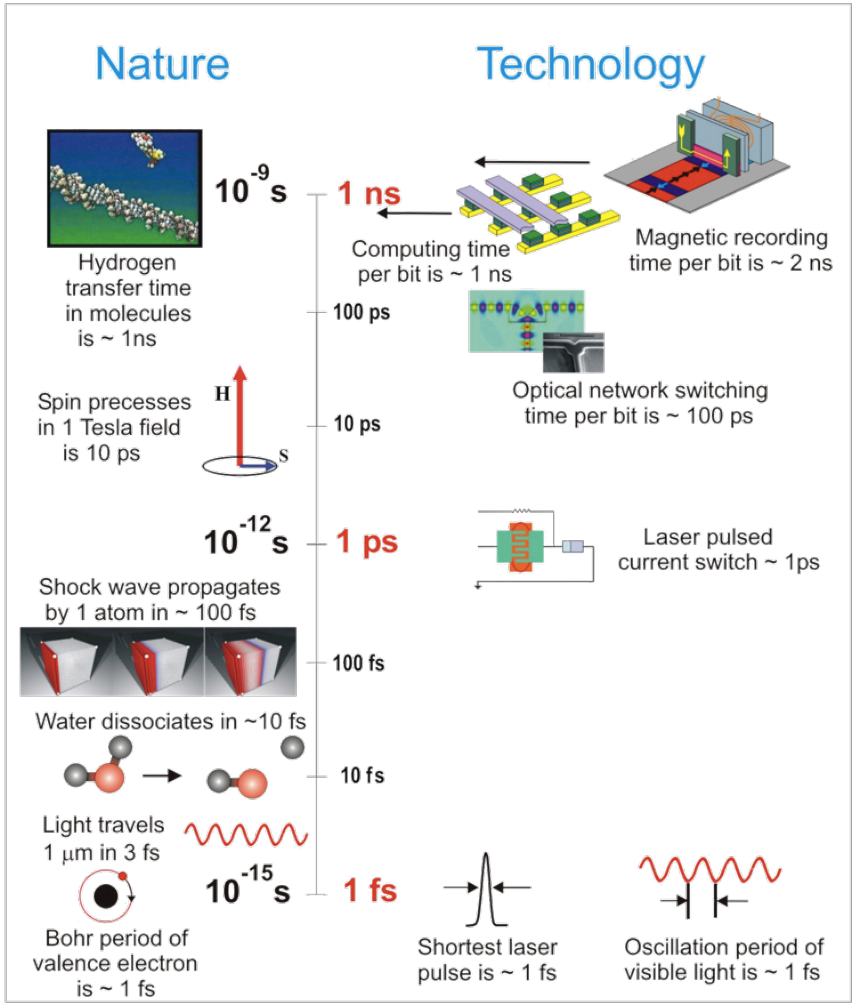

Time scales: smaller systems, shorter times.
At atomic scales, about 1Å, the time scales are fs.

UCLA

macro molecules

↓

molecular groups

↓

atoms

↓

"electrons" & "spins"

Nature		Technology
hummingbird wing motion ~ 1 ms	10^{-3} s — 1 ms	camera shutter speed ~ 130 μs
		flash ~ 30 μs
protein folding ~ 10 μs 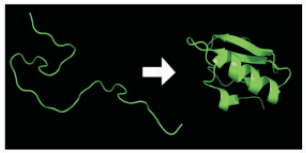	10^{-6} s — 1 μs	
molecular group motion ~ 1 ns 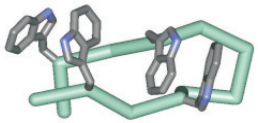	10^{-9} s — 1 ns	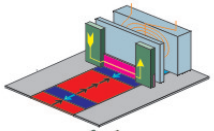 Magnetic recording time per bit ~ 1 ns
		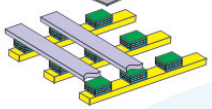 Computing time per bit ~ 100 ps
atoms oscillate in ~ 100 fs 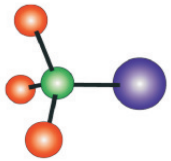	10^{-12} s — 1 ps	the technology gap
atomic electron circles in ~ 1 fs	10^{-15} s — 1 fs	optical laser pulse

Courtesy J. Stohr

Emission of Electromagnetic Radiation from free electrons

Electromagnetic waves can be generated in many ways, from transition between atomic energy levels in an atom or molecule, to acceleration or deceleration of charged particles, from particles moving faster than light in a medium or making a transition between two media with different index of refractions. One way of characterizing the emission is by dividing it in broad band or narrow band radiation and by the coherence properties.

Broad Band Radiation

- Synchrotron radiation
- Bremsstrahlung
- Transition radiation
- Diffraction radiation
- Cerenkov radiation

Narrow band radiation

- Oscillator radiation
- Smith-Purcell radiation
- Undulator radiation

For the generation of coherent, or laser, light we are interested in narrow band radiation sources.

Radiation by moving charges

UCLA

Lienard-Wiechert fields

J. D. Jackson, Classical Electrodynamics, 3rd ed. 1998.

$$\vec{E}(\vec{r},t) = \frac{e(\vec{n}-\vec{\beta}_e)}{\gamma^2 R^2 (1-\vec{n}\cdot\vec{\beta}_e)^3} + \frac{e\vec{n}\times[(\vec{n}-\vec{\beta}_e)\times\dot{\vec{\beta}}_e]}{cR(1-\vec{n}\cdot\vec{\beta}_e)^3}$$

$$\vec{R}(t') = \vec{r} - \vec{r}_e(t') \qquad t' = t - R(t')/c \qquad \vec{B}(\vec{r},t) = \vec{n}\times\vec{E}(\vec{r},t)$$

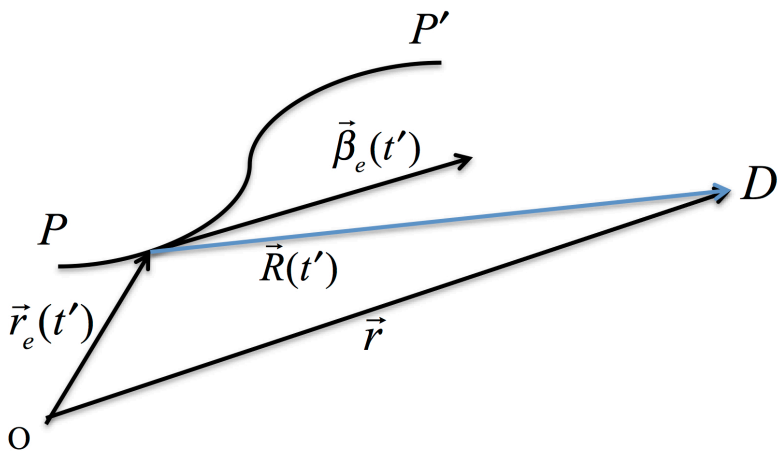

UCLA

Main characteristics of the radiation from moving charges

Power:

$$P = \frac{2r_e}{3c} mc^2 \gamma^6 [\dot{\vec{\beta}}^2 - (\vec{\beta} \times \dot{\vec{\beta}})^2]$$

Angular distribution:

$$\frac{dP}{d\Omega} = \frac{e^2}{4\pi c} \frac{\left| \vec{n} \times [(\vec{n} - \vec{\beta}) \times \dot{\vec{\beta}}] \right|^2}{(1 - \vec{n} \cdot \vec{\beta})^5}$$

Frequency angular distribution:

$$\frac{dI}{d\omega d\Omega} = \frac{e^2 \omega^2}{4\pi^2 c} \left| \int_{-\infty}^{\infty} \vec{n} \times (\vec{n} \times \vec{\beta}) e^{i\omega(t - \vec{n} \cdot \vec{r}(t)/c)} \, dt \right|^2$$

In all these expressions the velocity and acceleration are evaluated at the particle time. Notice that the expression for the frequency angular distribution does not contain the acceleration. If the acceleration is non zero only over a finite interval of time, say from t=0 to t=T, one has to add and subtract the integrals over the time when the velocity is constant, removing any ambiguity by inserting a convergence factor and taking the limit after evaluating the integral.

Spontaneous emission from an harmonic oscillator

UCLA

Let the oscillation be described by $\vec{r}_{os} = \vec{a}_0 \sin(\omega_0 t)$

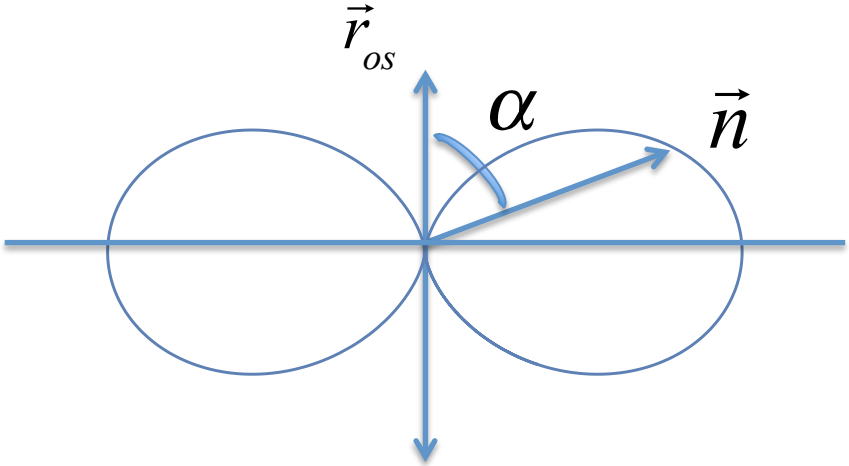

The radiation power angular distribution vanishes along the oscillation axis and is azimuthally symmetric about this axis.

$$\frac{dP}{d\Omega} = \frac{r_e mc^2 \omega_0^4 a_0^2}{8\pi c^3} \sin^2 \alpha$$

The power per unit frequency and solid angle at α =π/2, when the charge oscillates from t=0 to t=T is

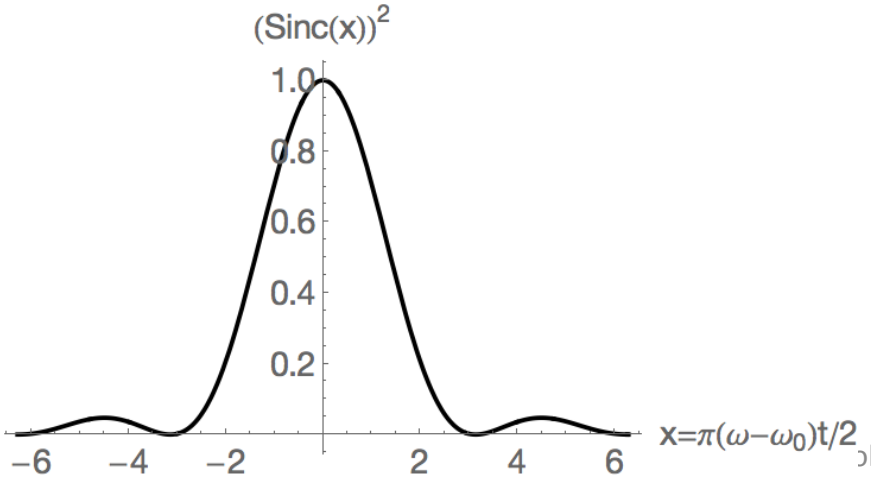

$$\frac{d^2 P}{d\omega d\Omega} = \frac{r_e mc^2 \omega_0^4 a_0^2 T}{8\pi^2 c^3} \left(\frac{\sin[(\omega - \omega_0)T/2]}{(\omega - \omega_0)T/2} \right)^2$$

Notice that the FWHM decreases with the oscillation time.

$$\Delta\omega / \omega_0 \approx 5.6 / \omega_0 T \approx (T_0 / T)$$

Doppler effect

- Assume the oscillator to be moving toward an observer with velocity βc along an axis perpendicular to the oscillation.
- The observer sees a Doppler shifted frequency and an angular distribution peaked forward

$$\omega' = \gamma\omega(1+\beta\cos\theta) \approx 2\gamma\omega \qquad \gamma = 1/\sqrt{1-\beta^2}$$

$$\tan\theta' = \frac{\sin\theta}{\gamma(\cos\theta+\beta)}, \quad \theta' \approx \frac{\theta}{2\gamma}$$

UCLA

X-ray FEL Physics: undulator radiation

X-ray FELs are based on the emission of electromagnetic waves from relativistic electrons moving in a periodic magnetic field, generating narrow band radiation.

H. Motz , Applications of the radiation from fast electron beams, J. Appl. Phys. 22, 527-535 (1951).

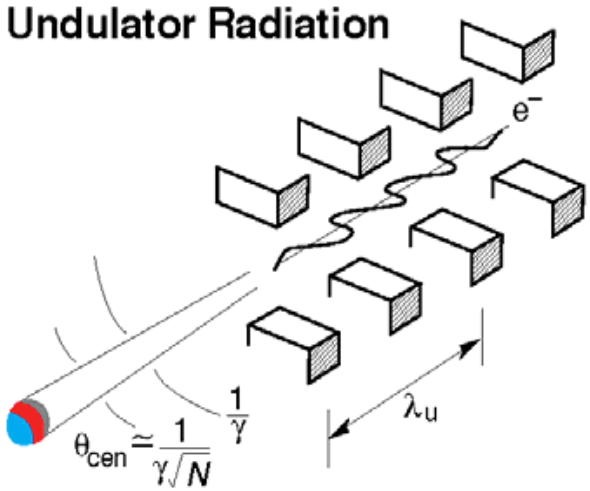

Basic FEL physics: undulator radiation from one electron

UCLA

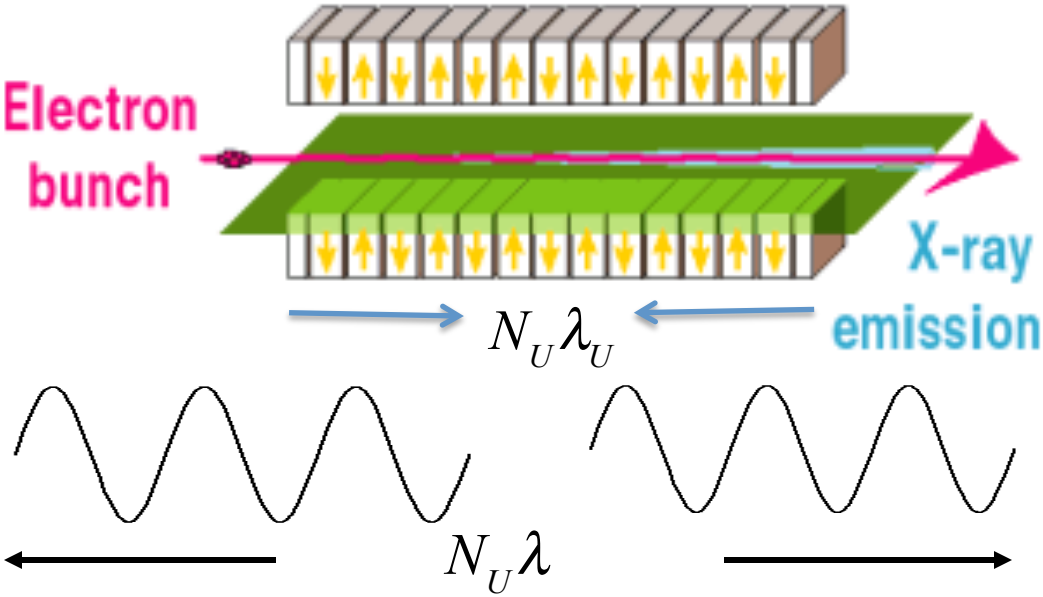

Each electron emits a wave train with N_U waves

Undulator with N_U periods.
The radiation is peaked at

$$\lambda = \lambda_U \frac{1+K^2/2}{2\gamma^2}$$

and the line width is

$$\Delta\lambda/\lambda \approx 1/N_U$$

$$K = \frac{eB_U\lambda_U}{2\pi mc^2} \approx 2-3$$

LCLS case: $\lambda_U = 3cm$, K=3, $\gamma = 3\times10^4$, $N_U = 3{,}300$

giving $\lambda \approx 1\,\mathring{A}$, $\Delta\omega/\omega = 3\times10^{-4}$, $N_U\lambda = 0.3\mu m$

UCLA

Why γ^2 ?

- If we go the electron frame where the longitudinal velocity is zero, the undulator appears as a plane wave with a period reduced by γ. In this frame the electron is an oscillator and emits radiation at a wavelength λ_U/γ
- Go back to the laboratory frame. The wavelength is shifted by another factor γ. Total γ^2.

Undulator radiation wavelength

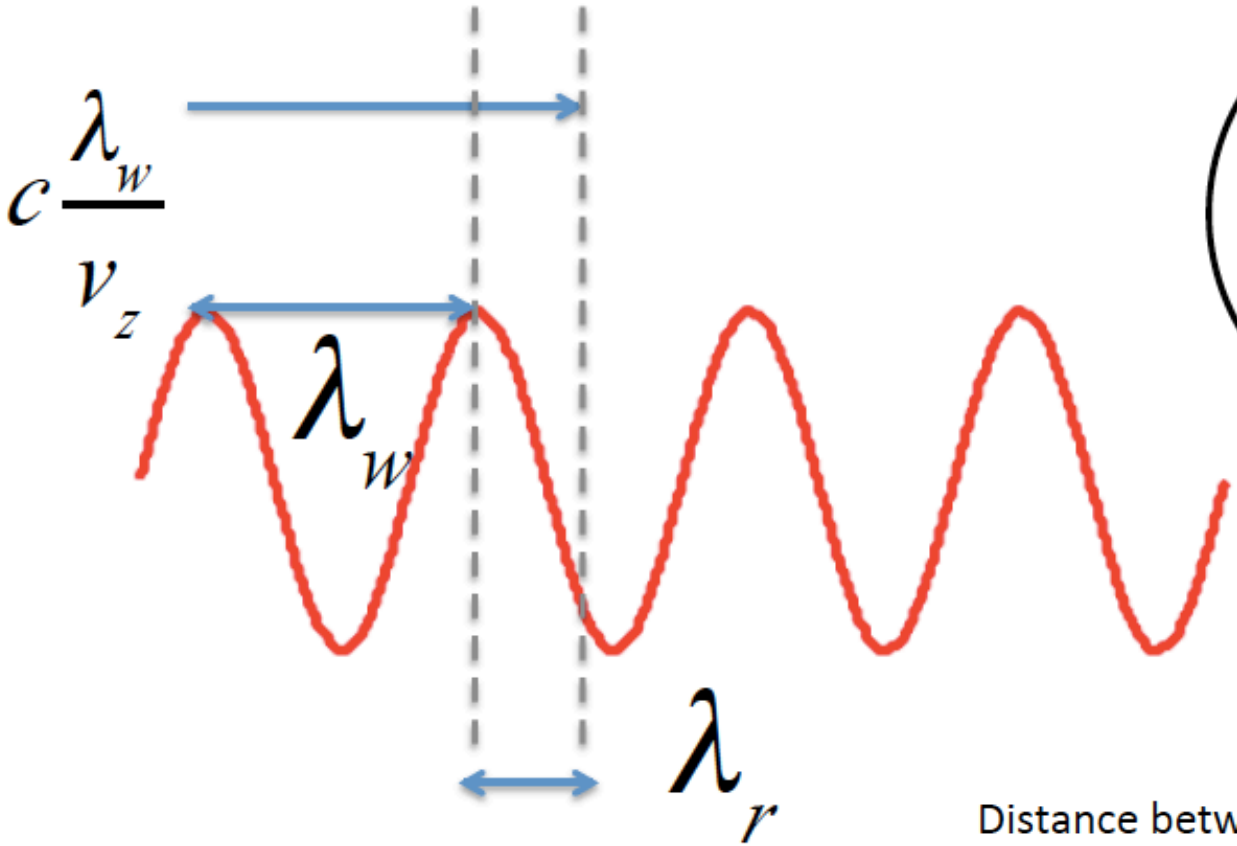

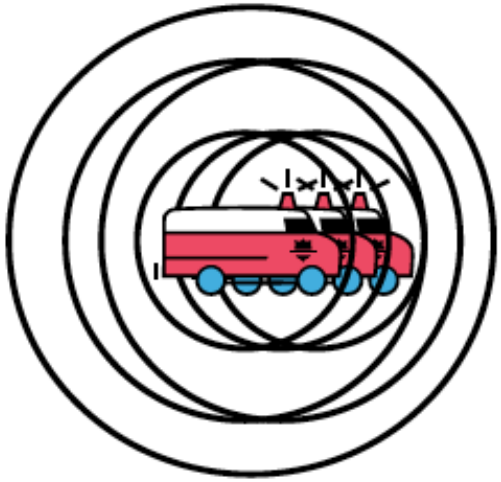

Dopppler shift of undulator period!

Distance between two consecutive wavefronts = wavelength

$$\lambda_r = \frac{\lambda_w}{\beta_z} - \lambda_w$$

Note: light slips ahead by 1 wavelength per oscillation period

Electron trajectory

UCLA

The two most common types of periodic undulator magnets are helical and planar undulators with constant period and peak magnetic field along the axis (Elleaume, Laser Handbook Vol.6, North Holland 1990). Electrons moving in a helical undulator produce circularly polarized radiation, while for planar undulator the radiation is plane polarized in the plane of the electron oscillations. We consider for simplicity helical undulator where the trajectory is a helix with constant longitudinal velocity

$$B_x = -B_0 \sin(k_U z),$$
$$B_y = B_0 \cos(k_U z),$$
$$B_z = -B_0 k_U [x \cos(k_U z) + y \sin(k_U z)].$$

$$\beta_{x0}(z) = \dot{x}_0 / c = -(K/\gamma)\sin(k_U z) \quad \beta_{y0}(z) = \dot{y}/c = (K/\gamma)\cos(k_U z) \qquad z_0 = \beta_z ct + z_0(0)$$

$$\beta_{z0} = \sqrt{1-(1+K^2)/\gamma^2} \simeq 1-(!+K^2)/2\gamma^2 \qquad a_{helix} = K / k_U \beta_{z0}\gamma$$

The expression for the velocity requires perfect initial values of position and velocity. Particles with different initial conditions will oscillate around this trajectory. In the planar case there is only one component of the transverse velocity and the longitudinal velocity is not constant.

E. Rutherford experiment, in 1909, using an alpha particle beam to "see" the structure of the atom.

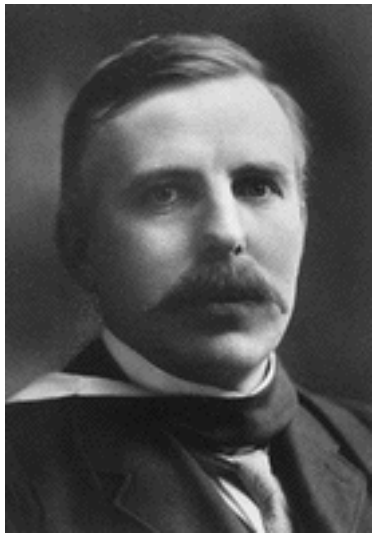

UCLA

[669]

LXXIX. *The Scattering of α and β Particles by Matter and the Structure of the Atom.* *By* Professor E. RUTHERFORD, *F.R.S., University of Manchester* *.

§ 1. IT is well known that the α and β particles suffer deflexions from their rectilinear paths by encounters with atoms of matter. This scattering is far more marked for the β than for the α particle on account of the much smaller momentum and energy of the former particle.

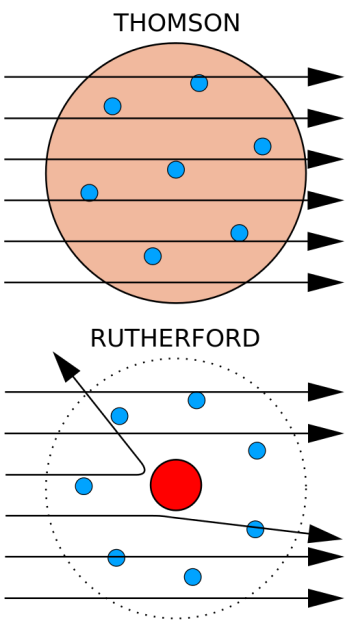

A "beam" of particles, having nearly the same momentum and same trajectory is needed to do the experiment.
The minimum observable scattering angle depends on the angular spread in the beam. The number of collisions observed increases with the transverse beam density. We would like to have a small beam radius and a small angular divergence.
Can we do it? What are the limitations?

Rutherford was able to put an upper limit on the radius of the gold nucleus of 34 femtometres. Present measures give for gold ~ 7.5 fm and for protons ~0.8 fm.

UCLA

Particle beam and phase space area

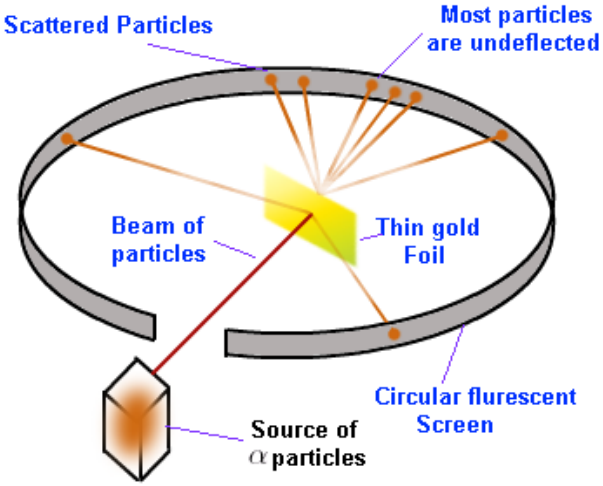

The ultimate limit is given by the uncertainty principle

$$\Delta x \Delta p_x \geq \hbar / 2$$

In the case of a beam we can make the approximation

$$p_z >> p_{x,y}, \ \theta \approx p_x / p_z \approx mc\gamma$$

To characterize how "good" is a beam we use the emittance or the normalized emittance

$$\varepsilon_T = \Delta x \theta \geq \hbar / 2mc\gamma = \lambda\!\!\!^{-}_c / \gamma \equiv \varepsilon_{T,N} / \gamma, \ \varepsilon_{NT} = \gamma \varepsilon_T$$

$\lambda\!\!\!^{-}_c \approx 3.8 \times 10^{-13} m$ is the reduced electron Compton wavelength

The best normalized emittance obtained from an electron source is about 10^{-7}m, well above the limit. Emittance is conserved in a linear transport system. Normalized emittance is conserved in a linear system, including acceleration.

Normalized emittance is an important figure of merit for electron sources. Preservation of emittances is critical for accelerator designs and their applications.

Light sources: visible light lasers, synchrotron radiation sources, X-ray lasers and more.

UCLA

The light from the Sun or from a conventional lamp, or an X-ray source like the one dentists are using consists of many colors, and is emitted in all directions, and at all times. These are incoherent sources.

For many scientific or medical uses we would like a monochromatic source, highly directional, and whose time duration can be controlled and can be made as short as that of the atomic processes we are studying.

We have again limits on the product of transverse position and momentum, energy and time duration. For a light source the phase space of coherent photons is given by:

$$\Delta x\theta \approx \lambda / 4\pi, \; c\Delta T\Delta\omega / \omega \approx \lambda / 4\pi$$

We can filter an incoherent source in position, angle and energy, as in the Rutherford experiment or in dentist office, at a cost of a corresponding loss in intensity. For a conventional light source the number of “coherent photons”, within the phase space limits is about one or smaller.

In a laser the number can very large. For our X-ray laser at SLAC, it is about 10^9.

Properties of laser beams: coherence, mono-chromaticity, directionality, brightness

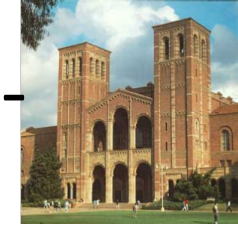

UCLA

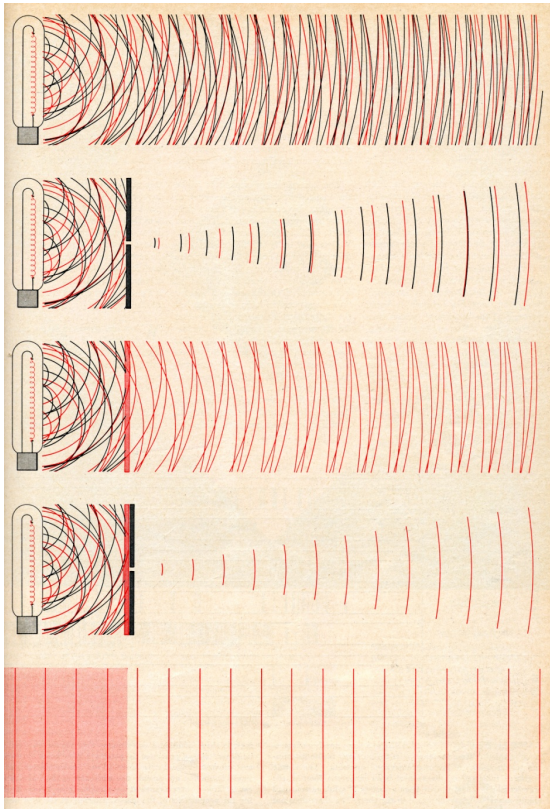

Starting from a black body like the Sun or any lamp we can obtain coherence, mono-chromaticity, directionality, by filtering. The result is low brightness, i.e. few photons.
The undulator does better because the radiation is peaked forward in a small angle ≈1/γ.

A. L. Schawlow "Laser Light"
Scientific American, 219 (3), p. 120, (1968)

UCLA

Retardation effects in undulator radiation

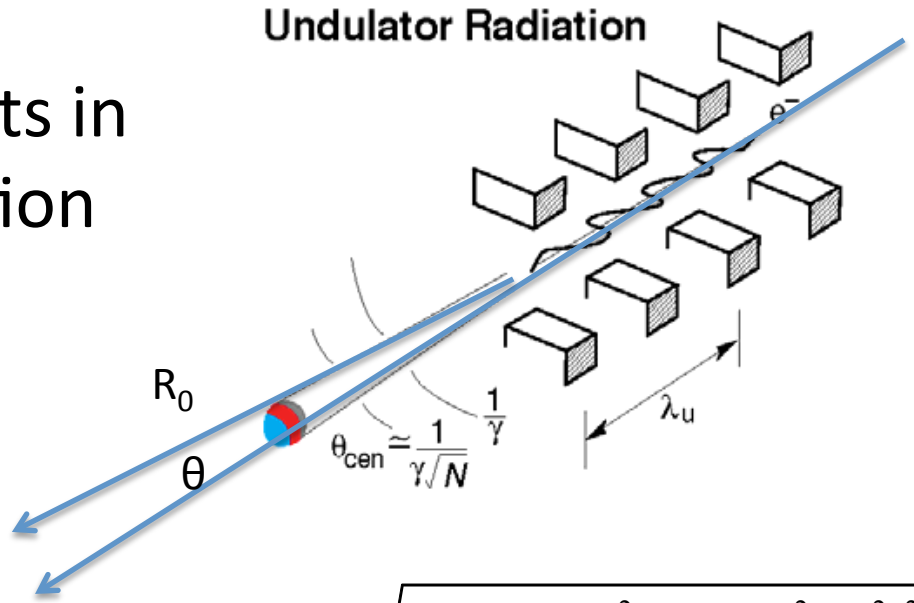

- Solve for the retarded time $ct' = \dfrac{ct - \beta_z R_0 - \sqrt{(ct-\beta_z R_0)^2 - (1-\beta_z^2)(c^2t^2 - R_0^2 - R_0^2\theta^2)}}{(1-\beta_z^2)}$

The difference in arrival time at the observer position of two wave fronts emitted at the undulator entrance and exit is given by

$$c\Delta T = N_U \lambda_U \left(\frac{1-\beta_z}{\beta_z} + \frac{\theta^2}{2} \frac{R_0}{R_0 - N_U \lambda_U} \right)$$

In the far field limit $c\Delta T = N_U \lambda_U \left(\dfrac{1-\beta_z}{\beta_z} + \dfrac{\theta^2}{2} \right)$

When the condition $c\Delta T = N_U \lambda$ is satisfied the waves emitted along the undulator have positive interference giving a peak in intensity at

$$\lambda = \lambda_U \left(\frac{1-\beta_z}{\beta_z} + \frac{\theta^2}{2} \right)$$

Slippage

- For the difference in velocity at the peak intensity wavelength the photon moves ahead of the electron emitting it by one wavelength per period. For the full undulator a photon emitted at the undulator entrance moves ahead by , a quantity called the slippage. The total slippage in the undulator is $S=N_U \lambda$, equal to the length of the wave train emitted by one electron.

Undulator radiation spectrum

The undulator radiation spectrum on axis is

$$\frac{d^2 I}{d\omega d\Omega} = \frac{2 r_e mc^2}{c} N_U^2 \gamma^2 \frac{K^2}{(1+K^2)^2} \left(\frac{\sin\Delta}{\Delta} \right)^2 \qquad \Delta = \pi N_U \left(\frac{\omega}{\omega_R} - 1\right)$$

The line width, FWHM, decreases with the undulator length $\frac{\Delta\omega}{\omega} \simeq \frac{2.8}{\pi N_U}$

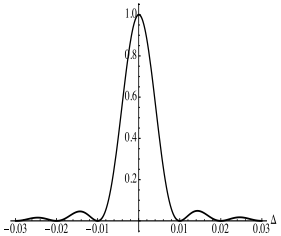

Off axis we also have the harmonics.

Coherent intensity and number of photons

- To evaluate the coherent intensity in the fundamental line we limit the angle to remain within the line width $1/N_U$

$$\theta_c = \sqrt{(1+K^2)/2\gamma^2 N_U} = \sqrt{\lambda/\lambda_U N_U} \qquad \Delta\Omega = \pi\theta_c^2 = \pi\lambda/\lambda_U N_U$$

Consider transversely coherent photons, $\sigma_r\,\theta_c = \lambda/4\pi$

The intensity is $$I_c = 2\pi^2 mc^2 \frac{r_e}{\lambda}\frac{K^2}{1+K^2} \qquad N_{ph,c} = \pi\alpha\frac{K^2}{1+K^2}$$

The number of photons emitted within the fundamental line width and the corresponding solid angle is a few times 10^{-2}. In a high gain FEL at 1A the number can be increased to 10^3.

Radiation from many, N_e, electrons. A picture of their emitted wave trains

UCLA

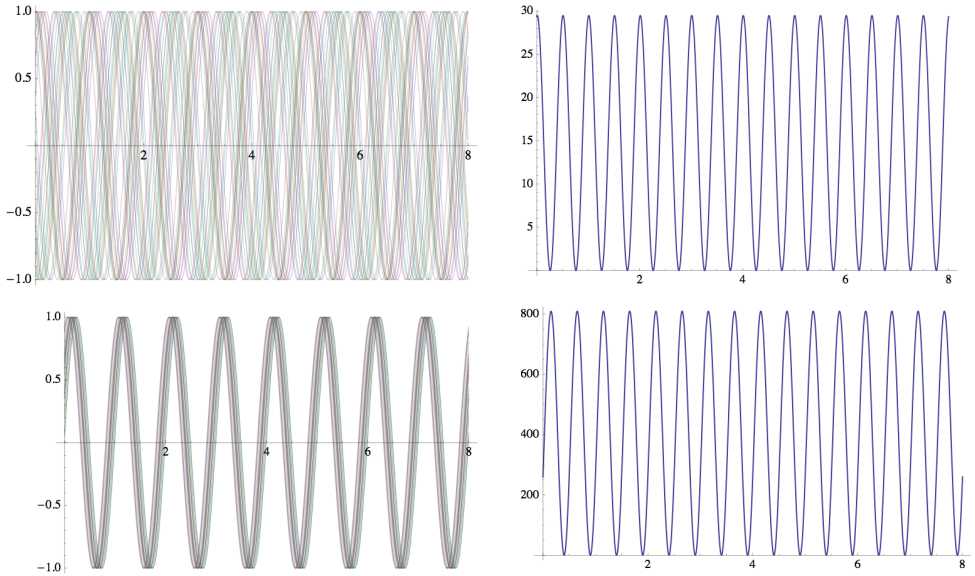

Disordered state, the single electron wave trains superimpose with random phases: noise. **Intensity ~ N_e**

Ordered state, all wave trains are in phase. **Intensity ~ N_e^2**

The order parameter is the "Bunching factor", *B*

$$B = \frac{1}{N_e}\sum_{n=1}^{N_e}\exp(i\phi_n)$$

Φ_n is the relative phase of the wave and the electron oscillation. *B=1* is perfect order.

N_e is about 10^9- 10^{10} . Large possible gain. Consider that at 1Å we have about 10^3 -10^4 electrons per wavelength. How do we squeeze them in one tenth of the wavelength and have these micro-bunching separated exactly by λ? How do we go from disorder to order? Answer: **FEL collective instability or self-organization effect.**

Important steps for the X-ray FEL: undulator radiation

UCLA

Hans Motz observed coherent radiation at Stanford at millimeter wavelength in 1953 using a planar undulator with 4 cm period and 3 to 5 MeV electron beam genrated by a linac with a bunch length shorter than the radiation wavelength. At 100 MeV he observed incoherent radiation. Using his words: " the mm wave generation might have some practical importance. In this case it is possible to bunch the electron beam so that groups of electrons radiate coherently. It was shown that the power level may be higher by a factor of the order of a million compared to non coherent radiation …"

(*Motz, H, W. Thon and R. N. Whitehurst, 1953,"Experiments on radiation by fast electron beams", J. Appl. Phys.* ***24****, 826)*

Can we do the same at wavelength of about 1Å? The answer is no, we do not know how to generate an electron beam with all electrons squeezed within λ/10 or separated by λ .

But in this case nature is kind to us. Under proper conditions, using an FEL the electron beam can go through a self-organization process and do just that, as we will see later.

FEL Collective Instability, a self-organization effect

UCLA

I. e-beam+undulator +EM field➔ electron energy modulation, scale λ;

$$\frac{d\gamma}{dt} \sim eE \bullet V_T \cos\Phi \qquad \Phi = \frac{2\pi}{\lambda}(z-ct) + \frac{2\pi}{\lambda_w} z$$

Φ is the relative phase of the field and electron oscillation. The energy modulation is large only when the phase is nearly constant. The wavelength is nearly the same of the spontaneous radiation.

$$\dot{\Phi} \approx 0, \ \lambda \approx \lambda_U (1+K^2)/2\gamma^2$$

Synchronism condition

II. energy modulation + undulator -> electron bunching, scale λ;

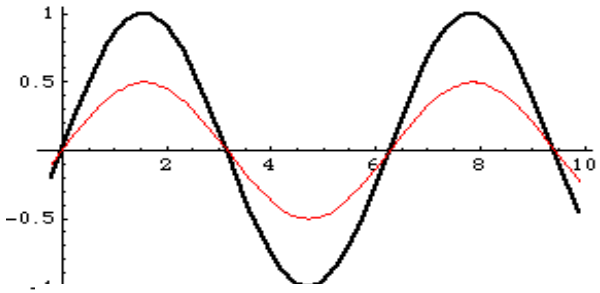

$$\frac{d\Phi}{dt} \sim \gamma - \gamma_0$$

III. larger bunching factor B -> higher EM field intensity ->go back to step I

COLLECTIVE INSTABILITIES AND HIGH-GAIN REGIME IN A FREE ELECTRON LASER

R. BONIFACIO *, C. PELLEGRINI
National Synchrotron Light Source, Brookhaven National Laboratory, Upton, NY 11973, USA

and

L.M. NARDUCCI
Physics Department, Drexel University, Philadelphia, PA 19104, USA

This effect is the equivalent of stimulated emission

Exponential power and micro-bunching growth

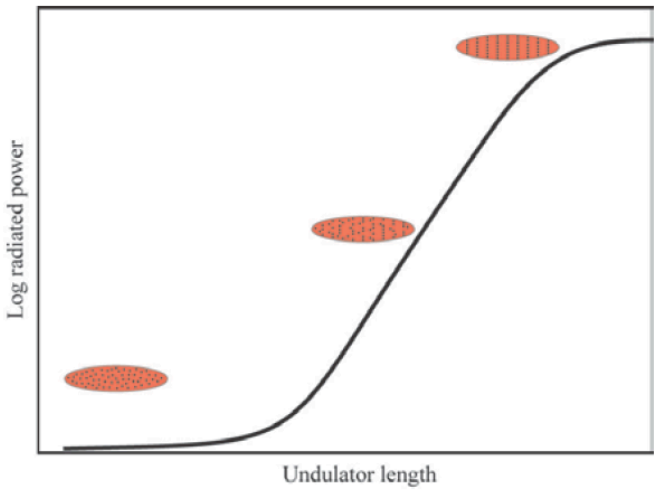

Good agreement of theory and experiments

2009 LCLS works

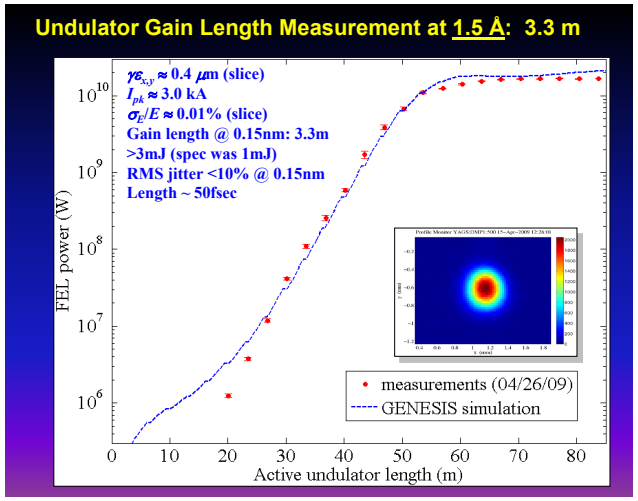

P. Emma et al., Nature Photonics 4, 641 (2010).

UCLA

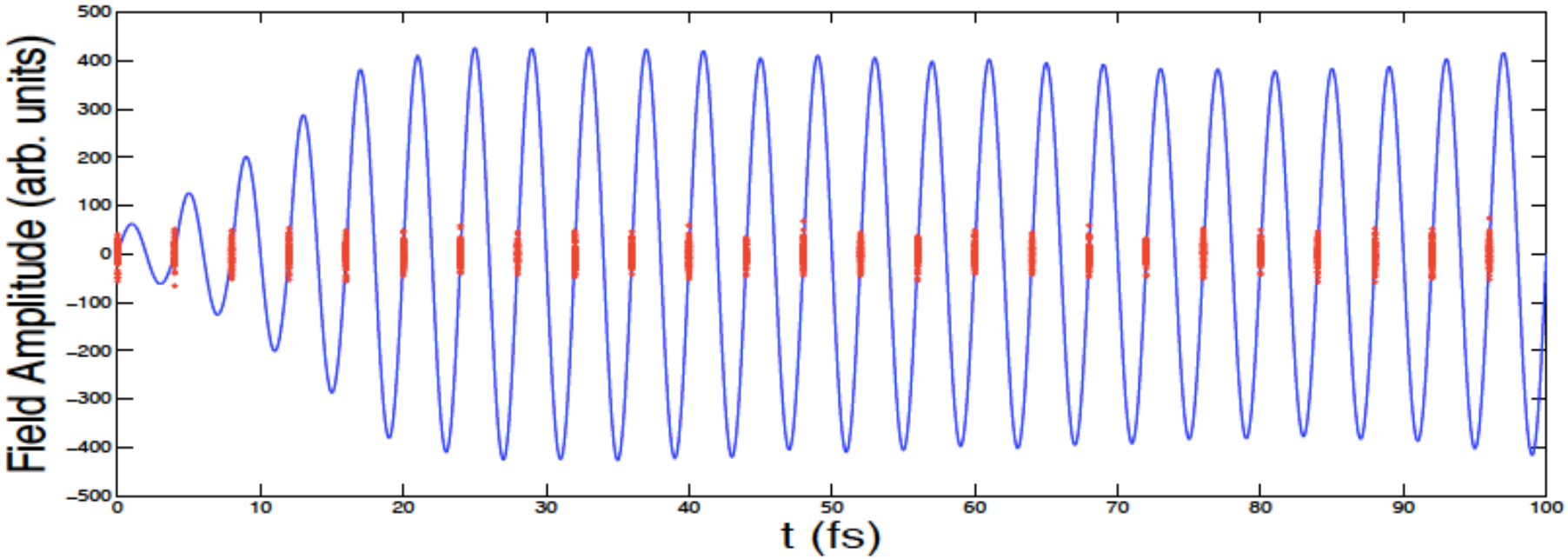

Particles are bunched at multiples of the wavelength.
Power is proportional to the square of the number of particles

FEL Collective Instability: main characteristics

UCLA

Universal FEL parameter	$\rho = \left(K\Omega_p / 4\gamma\omega_U \right)^{2/3}$
Gain Length	$L_G = \lambda_U / 4\pi\rho,$
Saturation power	$P_{sat} \simeq \rho P_{beam}$
Saturation length	$L_{sat} \simeq 10 L_G$
Line width	$\Delta\omega / \omega \simeq \rho$
Number of coherent photons/electron	$N_{ph,el} \simeq \rho E_{beam} / E_{ph}$

For the results to be valid we must have

$\sigma_{e,r}\sigma_{e,r} \leq \lambda_r / 4\pi,$ phase space matching

$\sigma_{e,E} < \rho,$ line width matching

$L_G < Z_R$ Gain>diffraction losses

Scaling: ρ scales as $\sqrt{\lambda}$, *very* good result.

For E_{ph}=10keV, E=15 GeV, $\rho=10^{-3}$, $N_{ph}\sim10^{3}$, compared to ~10^{-2} for spontaneous radiation, a gain of 5 orders of magnitude.

UCLA

Options for free electron lasers

SLAC

Easy

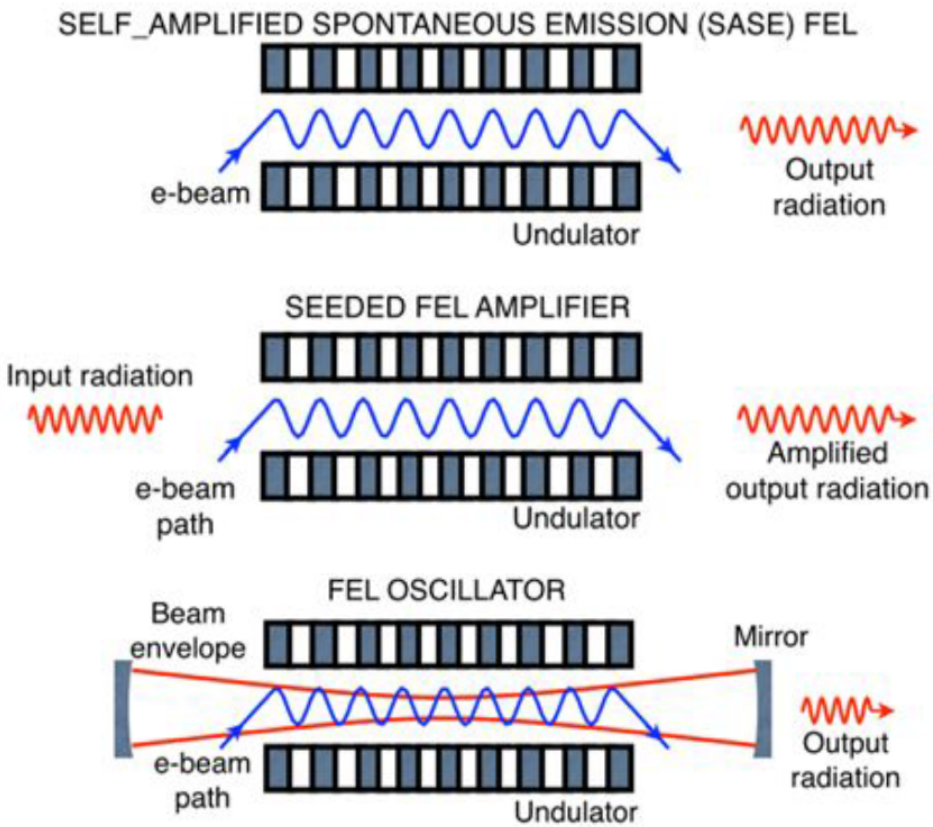

Hard

LCLS USA
SACLA Japan
FLASH Germany
XFEL Germany
SWISSFEL Switzerland
PAL FEL Korea

Hard X-rays, $E_{photon} \geq 5$keV

FERMI Italy
FLASH-II Germany
LCLS

Soft X-rays, $E_{photon} \leq 1$ keV

Proposal ANL USA

K.-J. Kim et al.

Brightness

- A convenient quantity to characterize the photon beam, is the **brightness**, defined using its six dimensional phase-space volume. Since the phase space volume is invariant under optical transformation the brightness is a good way to characterize a radiation source.
- The minimum transverse phase space volume for a diffraction limited photon beam is defined, for photons of wavelength λ, by $\Delta x \Delta\theta_x \geq \lambda/4\pi$, $\Delta y \Delta\theta_y \geq \lambda/4\pi$ (Siegman, Lasers, 1986). Considering a Gaussian photon beam and defining the transverse phase space as $2\pi\sigma_x \sigma_{\theta x} = \lambda/2$, the expression for brightness for a spatially coherent radiation source is

$$B_{ph} = \frac{N_{ph}}{(\lambda/2)^2 2\pi\sigma_t\sigma_\omega/\omega}$$

When the electron beam emittance is comparable to that of the photon beam the brightness is

$$B_{ph} = \frac{N_{ph}}{4\pi^2\Sigma 2\pi\sigma_t\sigma_\omega\omega} \qquad \Sigma = \sqrt{\sigma_x^2+\sigma_{rad}^2}\sqrt{\sigma_{x'}^2+\sigma_{rad'}^2}\sqrt{\sigma_y^2+\sigma_{rad}^2}\sqrt{\sigma_{y'}^2+\sigma_{rad'}^2}$$

Comparison of X-ray sources

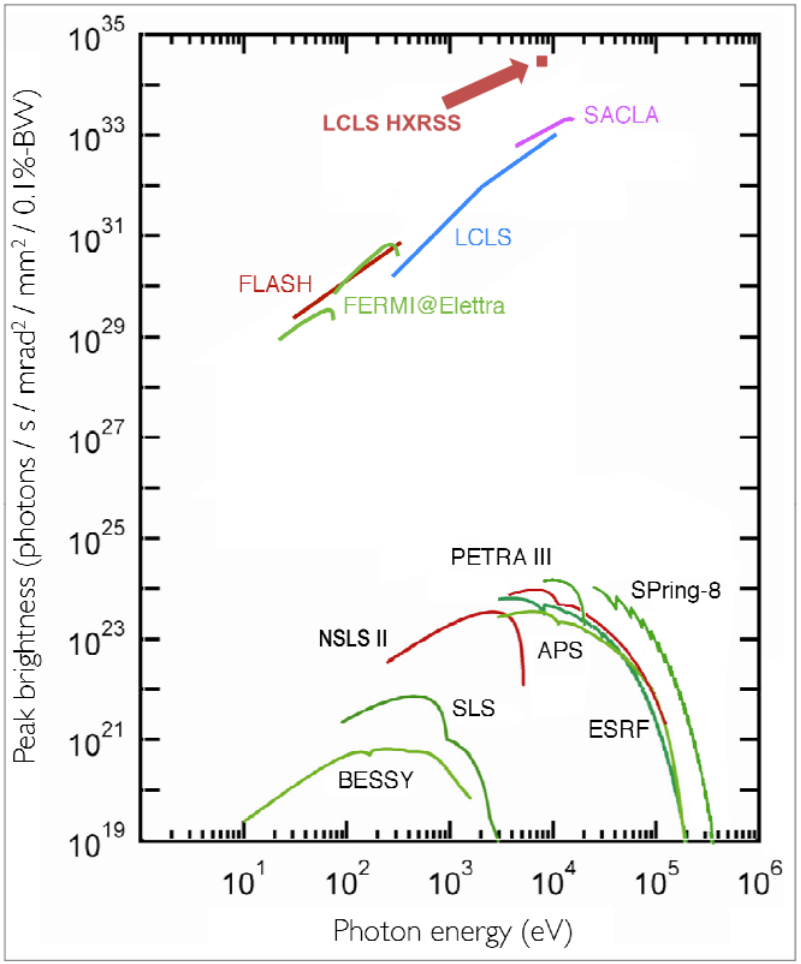

The best quantity to compare X-ray sources is the brightness, the number of photons in the X-ray beam six dimensional phase space. In practical units it is given by number of photons/sec/ $mm^2 mrad^2$/0.1% bandwidth. The plot shows the peak brightness for the most advanced X-ray sources, X-ray FELs and storage rings . Notice the jump by a factor 10^9 when LCLS started to operate in 2009.

Ref. Fletcher, L. B., et al., 2015, Nature Photonics **9**, 274.

Where does the factor 10^9 comes from?

A factor 10^5 comes from the increased number of photons/ electron.

Another factor comes from the pulse time duration, typically 10-100ps in storage ringsm compared to a few to 100 fs for X-ray FELs.

The last factor comes from the relative energy spread, about 10^{-3} in rings, smaller in X-ray FELs.

X-ray Free-electron Lasers

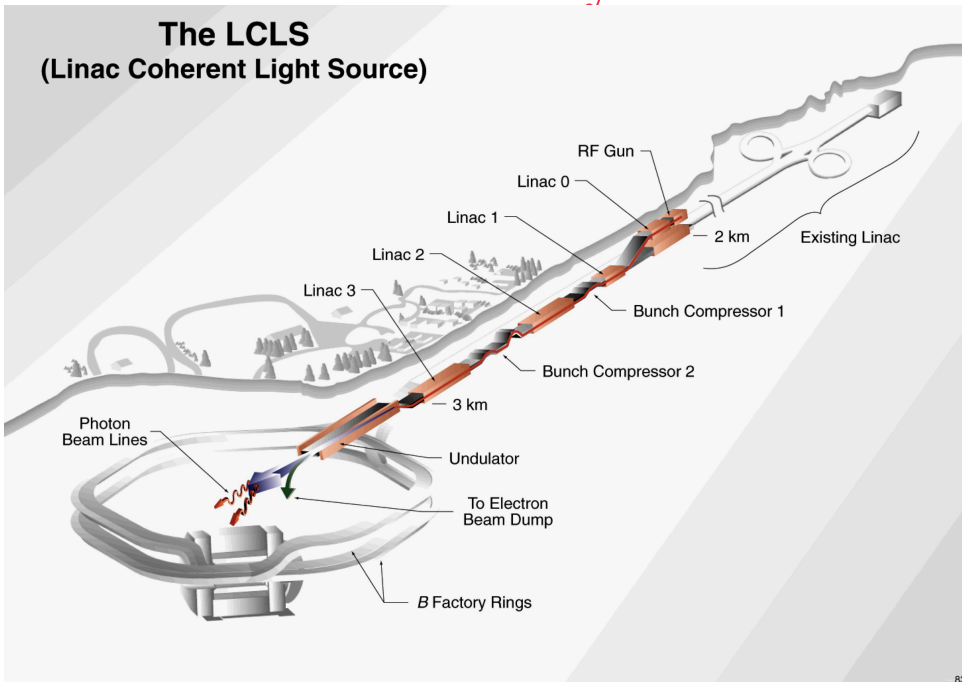

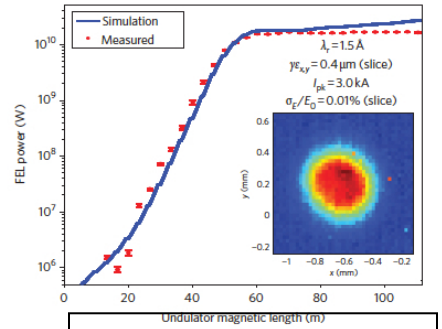

LCLS, 1.5 Å, 4/2009, 1-3 mJ

UCLA

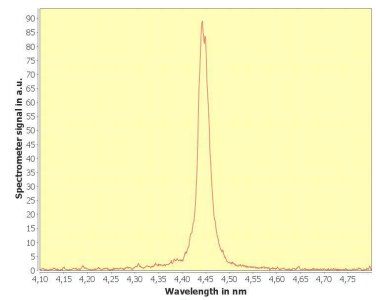

Flash: 4.45 nm, 0.3 mJ, 6/2010

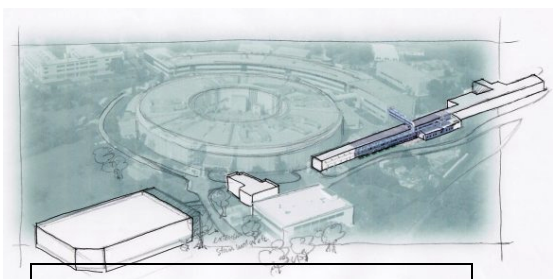

Fermi@Elettra, 43nm,12/2010

SACLA, 0.8 Å, 6/2011

New projects: European XFEL, LCLS-II, Swiss X-FEL, Korea X-FEL, Shanghai

X-ray FELs: Present Status

UCLA

Four X-ray FELs are in operation: LCLS at SLAC, SACLA in Japan, FLASH in Germany, Fermi in Italy, covering the wavelength range from 0.6A to 100 nm .

Swiss FEL, Korean FEL, European XFEL, LCLS-II are under construction and will start operation in the next two to three years.

General characteristics of X-ray pulses can be summarized as follows:

- ➔ Pulse energy hundreds of μJ to few mJ;
- ➔ Good transverse coherence
- ➔ Line width about 10^{-3} to 10^{-4}
- ➔ Pulse duration from a few to about 100 fs;
- ➔ About $2x10^{12}$ photons/pulse at 1Å, 100fs, more at longer wavelengths.
- ➔ Pulse repetition rate from about 100HZ to 10^5 to 10^6 for LCLS-II.

Linac Coherent Light Source at *SLAC*

A new era in x-ray sources and science

Proposed by C. Pellegrini in 1992
Lased April 10, 2009

1.5-15 Å
(14-4.3 GeV)

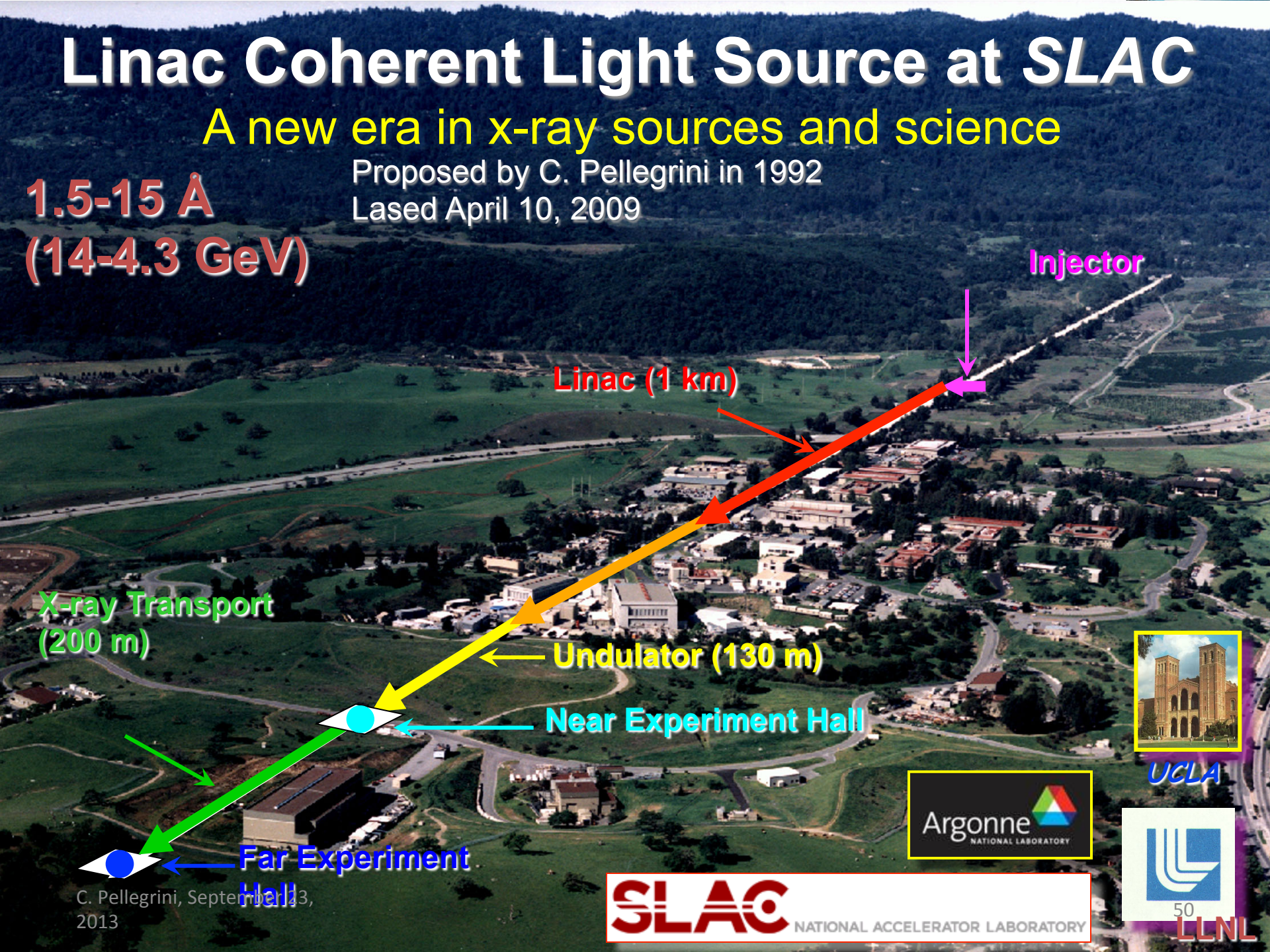

UCLA

The LCLS
(Linac Coherent Light Source)

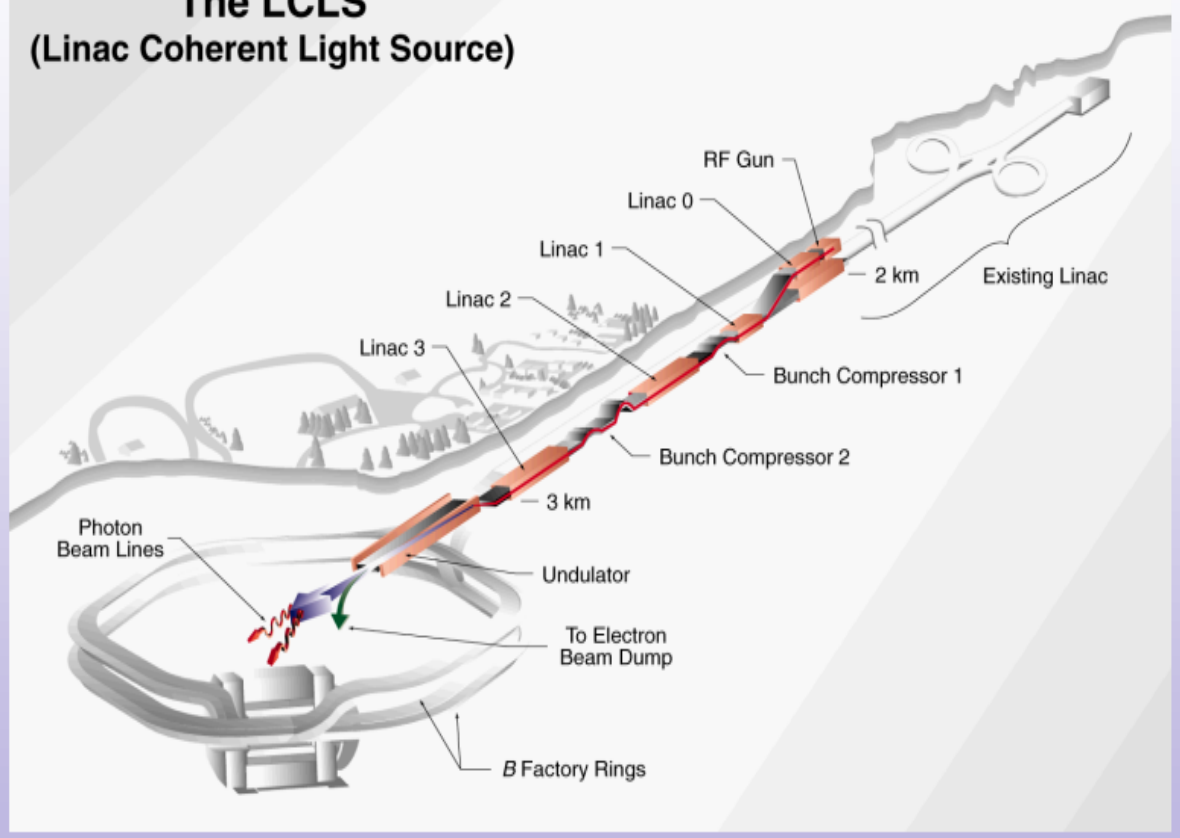

Stanford Linear Accelerator Center

SSRL

nsls

IR UV X

UCLA

LLNL

ADVANCED PHOTON SOURCE

Los Alamos
science serving society

LCLS: the world's first x-ray free electron laser

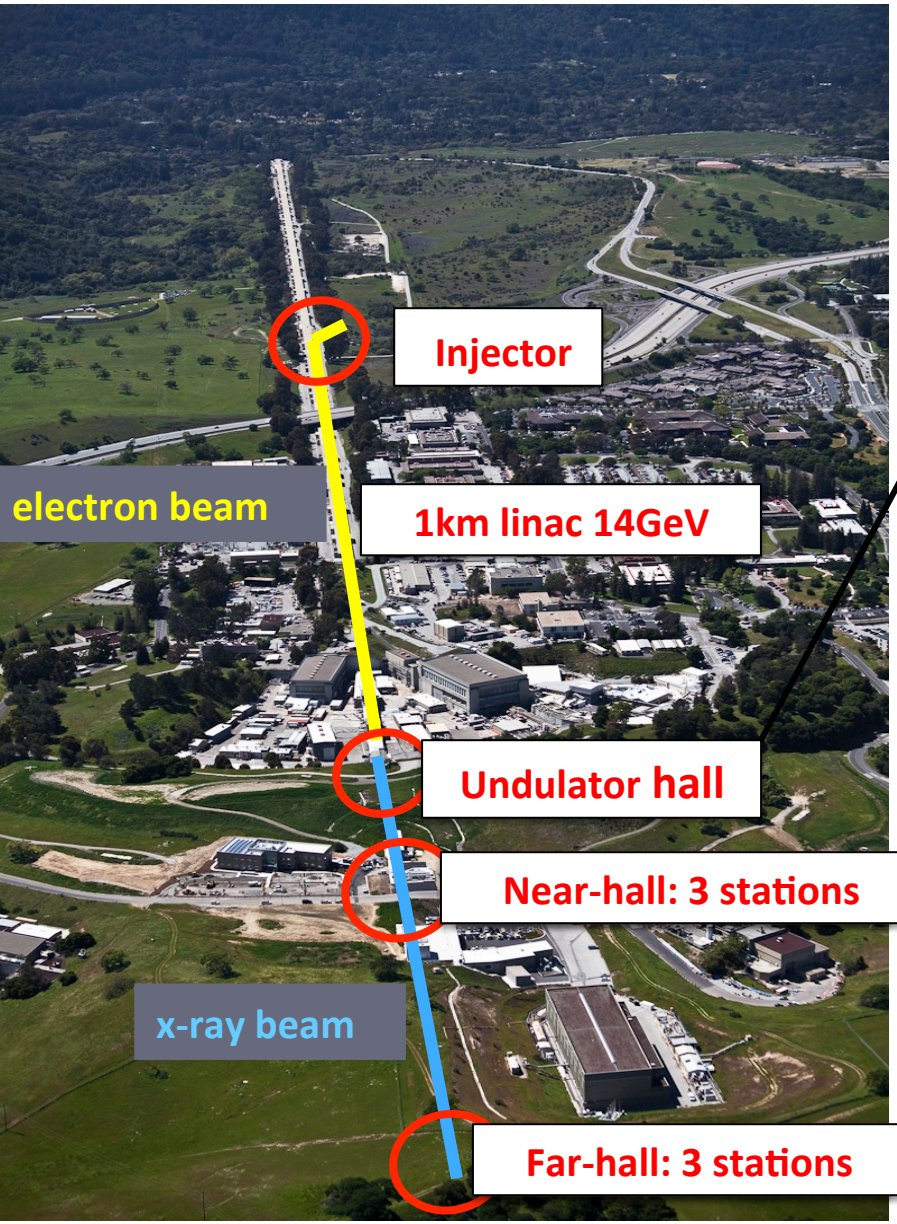

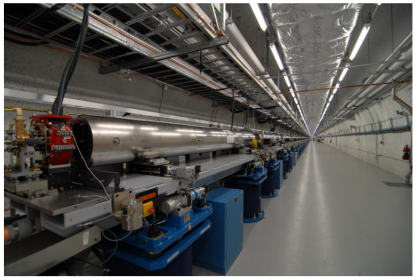

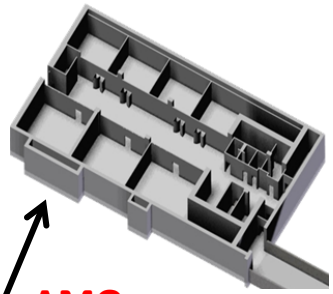

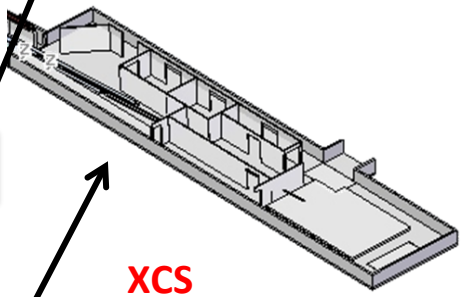

UCLA

- AMO: Atomic, Molecular & Optical Science
- CXI: Coherent X-ray Imaging
- MEC: Matter in Extreme Conditions
- SXR: Soft X-ray Materials Science
- XCS: X-ray Correlation Spectroscopy
- XPP: X-ray Pump Probe

More instruments will be added with LCLS II, starting about 2018.

Remarks on 4th generation

UCLA

•FLASH, Fermi, SACLA and LCLS have demonstrated outstanding capabilities, increasing by 7 to 9 orders of magnitude the photon peak brightness.

•The LCLS X-ray pulse duration and intensity can be changed from about 100 to a few femtosecond and 10^{13} to 10^{11} photons/pulse, over the wavelength range of 4 to 0.12 nm, by varying the electron bunch charge from 250 to 20 pC. **The X-ray pulse wavelength, intensity and duration can be optimized for each experiment, something not possible in storage ring sources**.

UCLA

Characteristics of hard X-ray FELs in operation or under construction.

	LCLS	SACLA	European XFEL*	Korean X-FEL*	Swiss X-FEL*	LCLS-II Cu RF
Electron energy, GeV	2.15-15.9	5.2-8.45	8.5-17.5	4-10	2.1-5.8	2.5 - 15
Wavelength range, nm	0.11-4.4	0.275-0.063	5.1-0.04	0.6-0.1	7-0.1	1.2 – 0.05
X-ray pulse energy, mJ	1-3 for $0.1<\lambda<1.5$	0.2-0.4 for $0.08<\lambda<0.275$	0.67-8.5 for $0.04<\lambda<5.1$	0.81-1 for $0.1<\lambda<0.6$nm	0.5-1.3 for $0.1<\lambda<7$	1-4.5 for $0.05<\lambda<0.4$
Pulse duration, rms, fs	5-250 for $0.1<\lambda<1.5$	4.3 for $0.08<\lambda<0.275$	1.68-107 for $0.04<\lambda<5.1$	8.6-26 for $0.1<\lambda<0.6$nm	2-20 for $0.1<\lambda<7$	5-50
Line width, rms, % SASE	0.5-0.1 for $0.1<\lambda<1.5$	0.11-0.37 for $0.08<\lambda<0.275$	0.02-0.25 for $0.04<\lambda<5.1$	0.15-0.18 for $0.1<\lambda<0.6$nm	0.06-0.4 for $0.1<\lambda<7$	0.2-0.1
Line width, rms,% seeded	0.01-0.005 for $0.1<\lambda<1.5$	0.01-0.03* $0.08<\lambda<0.275$	0.04-0.005 for $0.04<\lambda<5.1$	0.002 -0.002 for $0.1<\lambda<0.6$nm	0.01-0.002 for $0.1<\lambda<7$	0.02

Characteristics of Soft X-ray FELs operating and under construction. LCLS-II has two undulators, SXR and HXR.

	FLASH	Fermi FEL-1	Fermi FEL-2	LCLS-II SXR Und.	LCLS-II HXR Und.
Electron energy, GeV	0.35-1.25	1.0 - 1.5		3.6 – 4.0	3.3 – 4.0
Wavelength range, nm	52-4.2	100-20	20-4	6 – 1.0	1.2 – 0.25
X-ray pulse energy, mJ	0.2 @ λ_{Max}, 0.5 @ λ_{min}	0.3 @ λ_{Max}, 0.1 @ λ_{min}	0.1 @ 10.8 nm, 0.01 @ λ_{min}	0.9 @ λ_{max}, 0.4 @ λ_{min}	1.1 @ λ_{max}, 0.02 @ λ_{min}
Pulse duration, rms, fs	15-100 @ λ_{Max} 15-100 @λ_{min}	Depending on seed pulse duration and harmonic order, typically 40-100		6 - 50	6 - 50
Line width, rms, % SASE	0.2 @ λ_{Max} 0.15 @λ_{min}			0.1	0.2 – 0.05
Line width,rms, % seeded		0.06 @λ_{Max} 0.03 @ λ_{min}	0.06@10.8nm, 0.02@5.4nm, 0.04@λ_{Min}	0.02	--

An important characteristic of LCLS-II is the very high repetition rate up 0.1 to 1 MHz, made possible by the use of superconducting, CW, linac.

Single-shot Young's double slit measurements on LCLS x-ray beam

UCLA

PRL **107,** 144801 (2011) PHYSICAL REVIEW LETTERS week ending 30 SEPTEMBER 2011

Coherence Properties of Individual Femtosecond Pulses of an X-Ray Free-Electron Laser

I. A. Vartanyants,[1,2,*] A. Singer,[1] A. P. Mancuso,[1,†] O. M. Yefanov,[1] A. Sakdinawat,[3] Y. Liu,[3] E. Bang,[3] G. J. Williams,[4] G. Cadenazzi,[5] B. Abbey,[5] H. Sinn,[6] D. Attwood,[3] K. A. Nugent,[5] E. Weckert,[1] T. Wang,[4] D. Zhu,[4] B. Wu,[4] C. Graves,[4] A. Scherz,[4] J. J. Turner,[4] W. F. Schlotter,[4] M. Messerschmidt,[4] J. Lüning,[7] Y. Acremann,[8] P. Heimann,[9] D. C. Mancini,[10] V. Joshi,[10] J. Krzywinski,[4] R. Soufli,[11] M. Fernandez-Perea,[11] S. Hau-Riege,[11] A. G. Peele,[12] Y. Feng,[4] O. Krupin,[4,6] S. Moeller,[4] and W. Wurth[13]

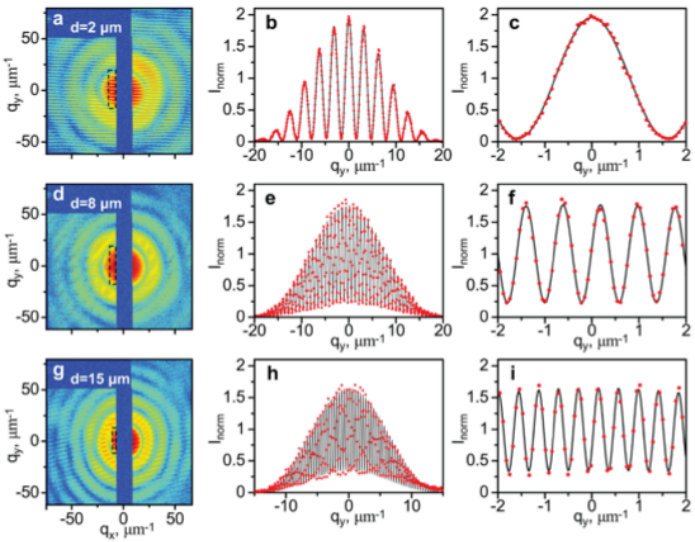

Transverse coherence quite good, the X-ray beam is diffraction limited, in agreement with theory. Spatial coherence is essential for applications like coherent x-ray diffractive imaging, x-ray holography and x-ray photon correlation spectroscopy. The recovery of structural information from coherent imaging experiments relies on a high degree of spatial coherence in the incident field to enable the phasing of the diffraction pattern produced by its scattering from the sample.

Time dependent effects

The spectral properties of a SASE FEL and the spiky nature of the radiation are due to the start from noise and to slippage: photons are faster than electrons and slip ahead by one wavelength per undulator period. The length over which the radiation from one electron interacts with other electron is the slippage in one gain length, or cooperation length the cooperation length

$$L_C = \lambda_r / 4\pi\rho$$

FEL Collective Instability: causality

UCLA

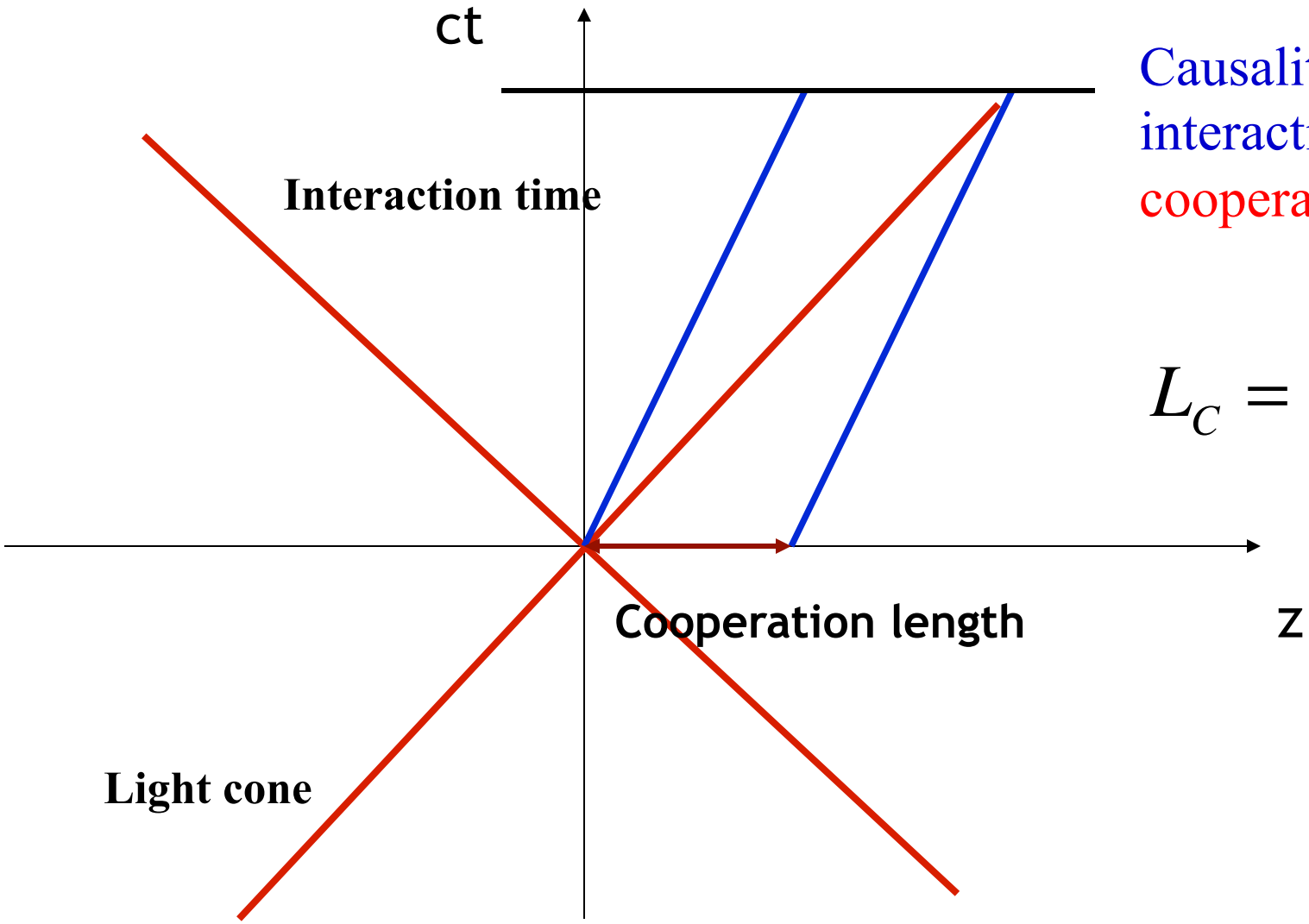

Causality limits the interaction to the cooperation length:

$$L_C = \frac{\lambda}{4\pi\rho}$$

UCLA

Time dependent effects

VOLUME 73, NUMBER 1 PHYSICAL REVIEW LETTERS 4 JULY 1994

Spectrum, Temporal Structure, and Fluctuations in a High-Gain Free-Electron Laser Starting from Noise

R. Bonifacio,[1,2] L. De Salvo,[1] P. Pierini,[2] N. Piovella,[1] and C. Pellegrini[3]

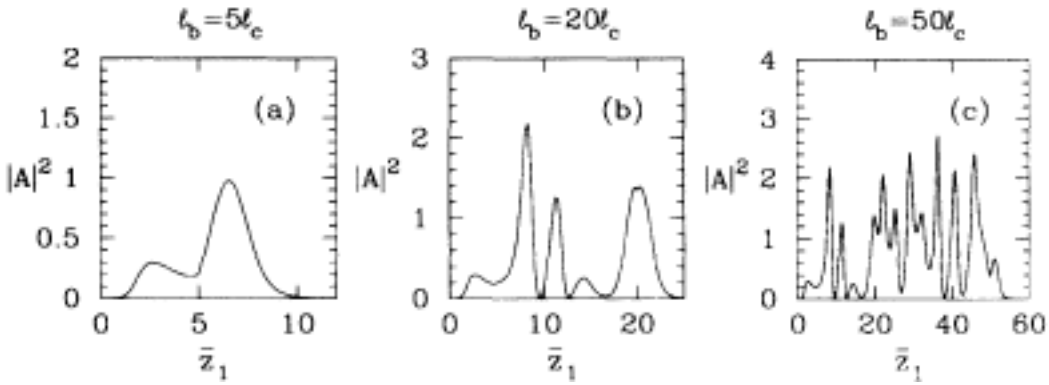

Temporal profile for different ratios of bunch length to cooperation length.

Improving LCLS temporal coherence: Self-seeded spectra

Self-seeding is a way to improve the spectrum and reduce the line-width using the transmission around the stop band of a Bragg reflection in a diamond crystal, Geloni, G., V. Kocharyan and E. Saldin, 2011, Journal of Modern Optics **58,** 16.

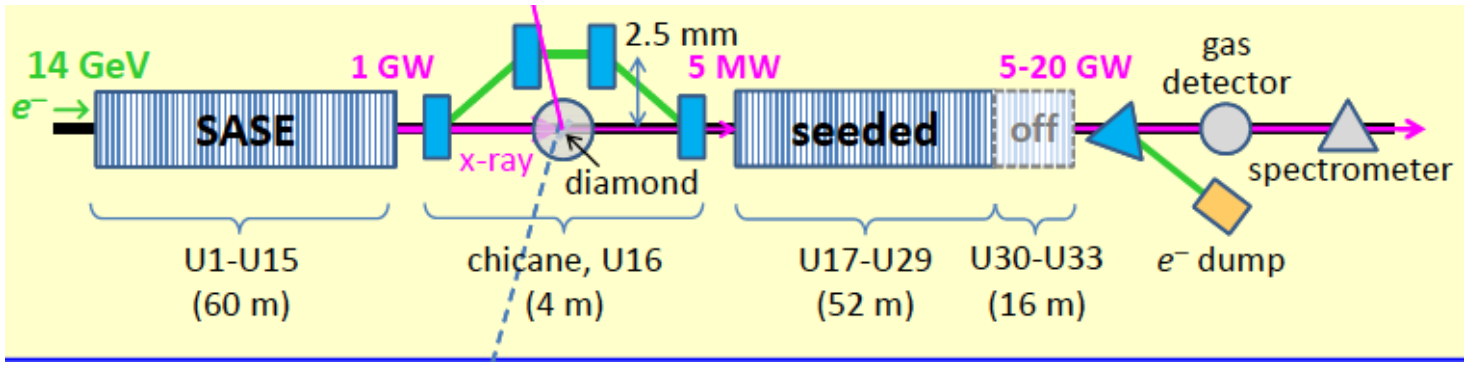

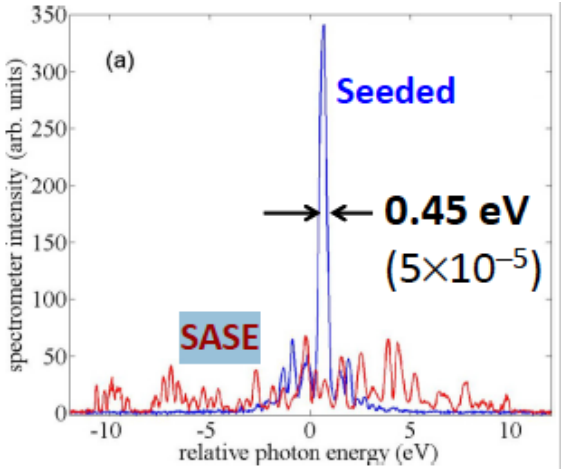

The concept as been demonstrated at LCLS , J. Amann, et al. Nature Photonics, DOI: 10.1038/NPHOTON 2012.180

Twin-Bunch FEL

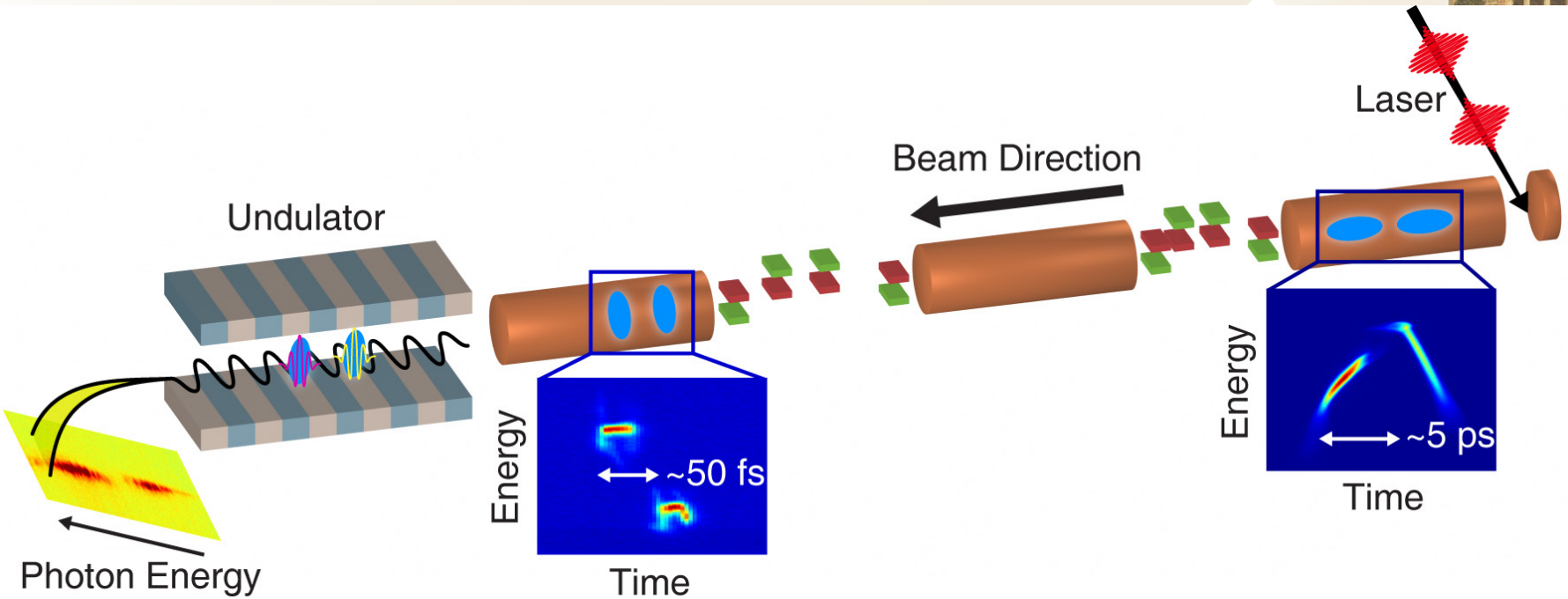

ARTICLE

Received 16 Oct 2014 | Accepted 22 Jan 2015 | Published 6 Mar 2015

DOI: 10.1038/ncomms7369 OPEN

High-intensity double-pulse X-ray free-electron laser

A. Marinelli[1], D. Ratner[1], A.A. Lutman[1], J. Turner[1], J. Welch[1], F.-J. Decker[1], H. Loos[1], C. Behrens[1,2], S. Gilevich[1], A.A. Miahnahri[1], S. Vetter[1], T.J. Maxwell[1], Y. Ding[1], R. Coffee[1], S. Wakatsuki[1,3] & Z. Huang[1]

nature COMMUNICATIONS

High-intensity double-pulse X-ray free-electron laser

A. Marinelli1, et al., Nature Comm., DOI: 10.1038/ncomms7369

UCLA

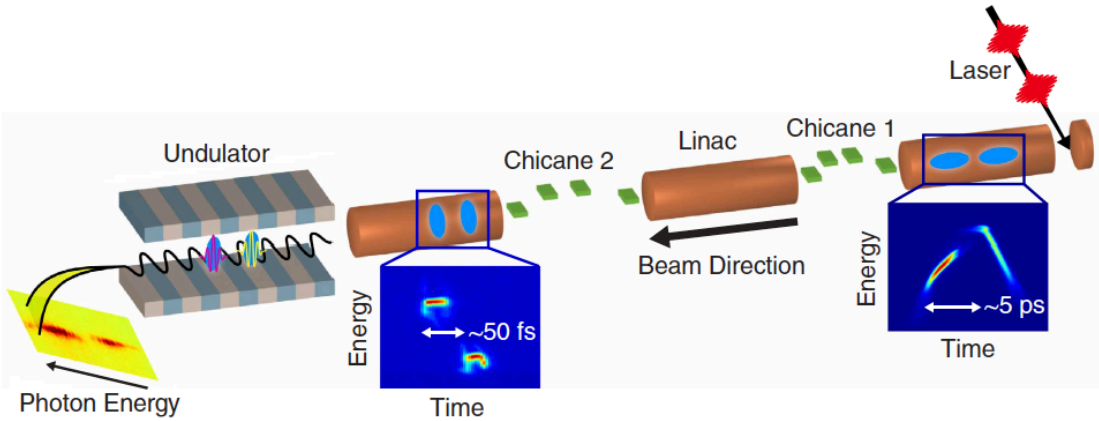

Double laser pulse on cathode generates two electron bunches separated in time, 0-100 fs, and energy,~100eV. Average photon energy 8.3keV. Used in pump-probe experiments.

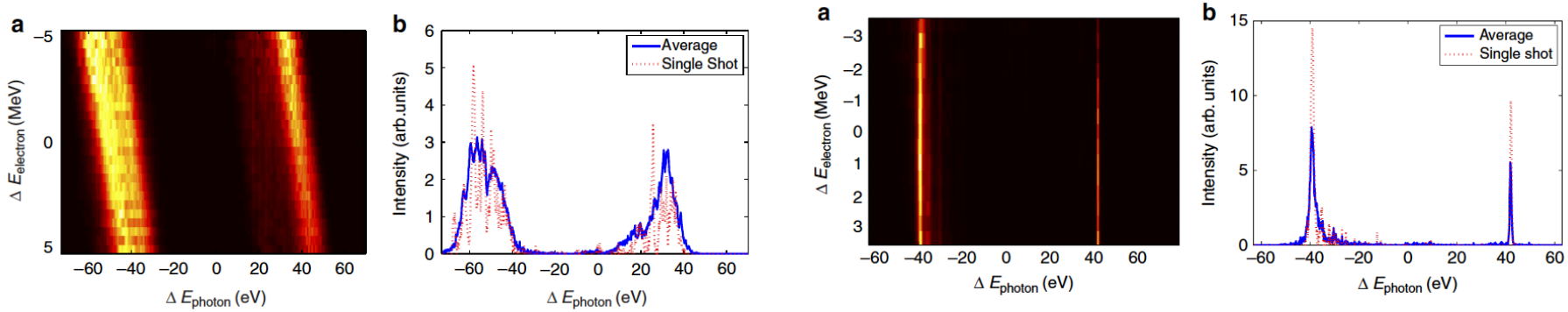

Spectral measurements: SASE, left; self-seeding, right. (a) Intensity as a function of beam energy and photon energy (b) Average and single-shot for fixed beam energy.

Time Delay Control for X-Ray Pump/X-Ray Probe Experiments

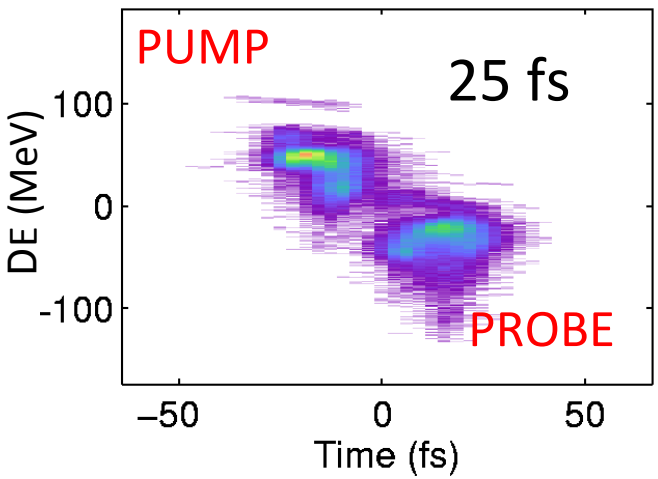

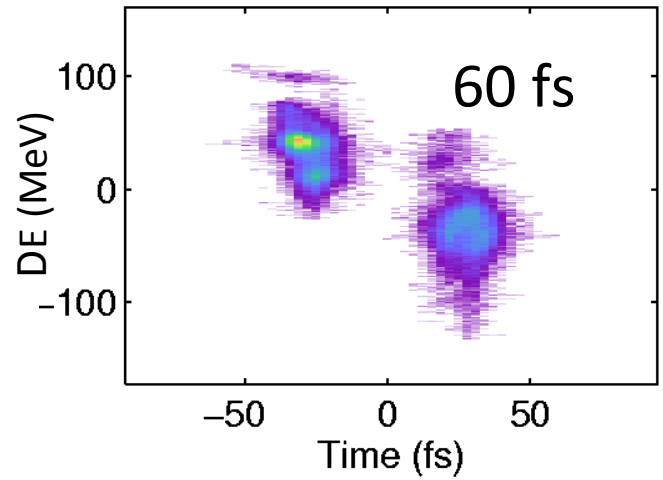

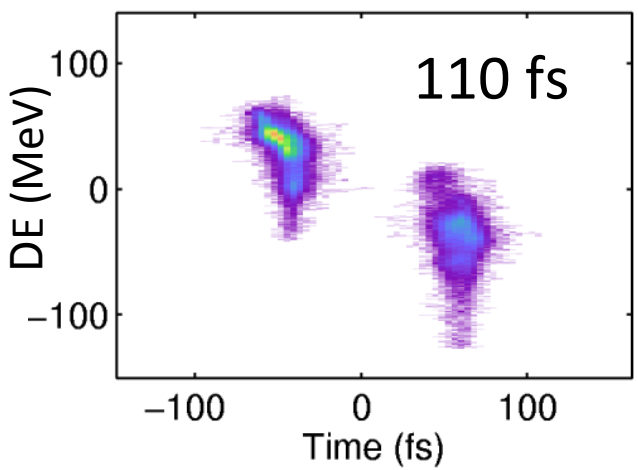

$$\Delta T_{final} = \frac{\Delta T_{initial}}{C_{factor}} + \Delta T_{GAP} \times \frac{1}{E}\frac{dE}{dt}_{wakes} \times \frac{R56}{c}$$

Twin-Bunch FEL

- Using the two-bunch two colors technique in a pump probe configurations with 0 to 100 fs variable delay, S. Boutet et al. have recently imaged in great detail molecular radiation damage. (S. Boutet, private communication)

Imaging Molecular Damage at the fs Time-Scale

Courtesy of S. Boutet

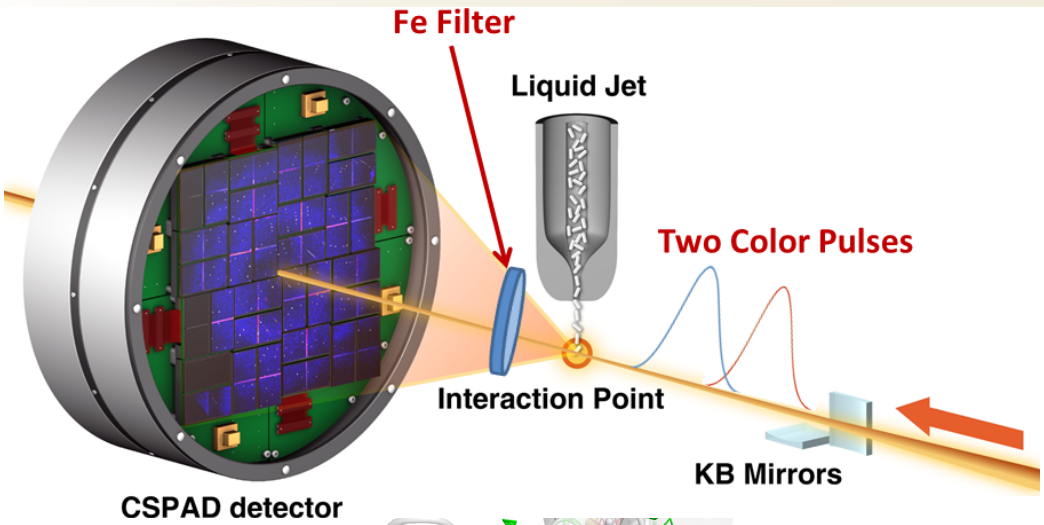

High-Energy pump absorbed by filter.
Low-energy probe goes through.
Use short pulses (~10-15 fs)
Vary delay and look at difference electron density maps.

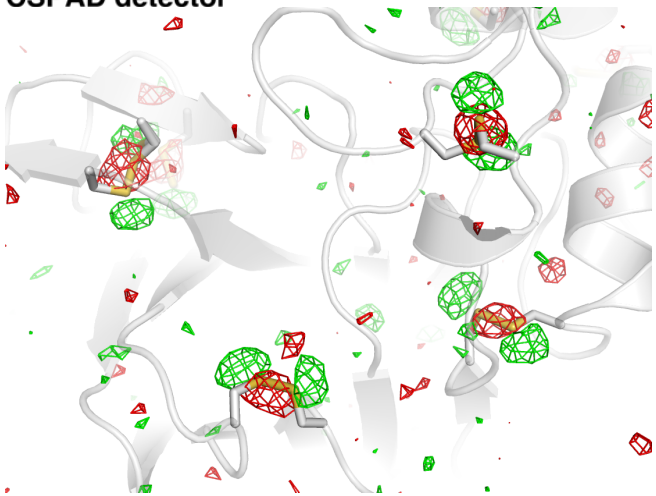

Thaumatin Molecule

Difference between unperturbed sample and pump-probe (100 fs delay).

Green: positive electron density
Red: negative electron density

Movie of Molecular Explosion

Courtesy S. Boutet

Vary time-delay to make a "movie" of the process.

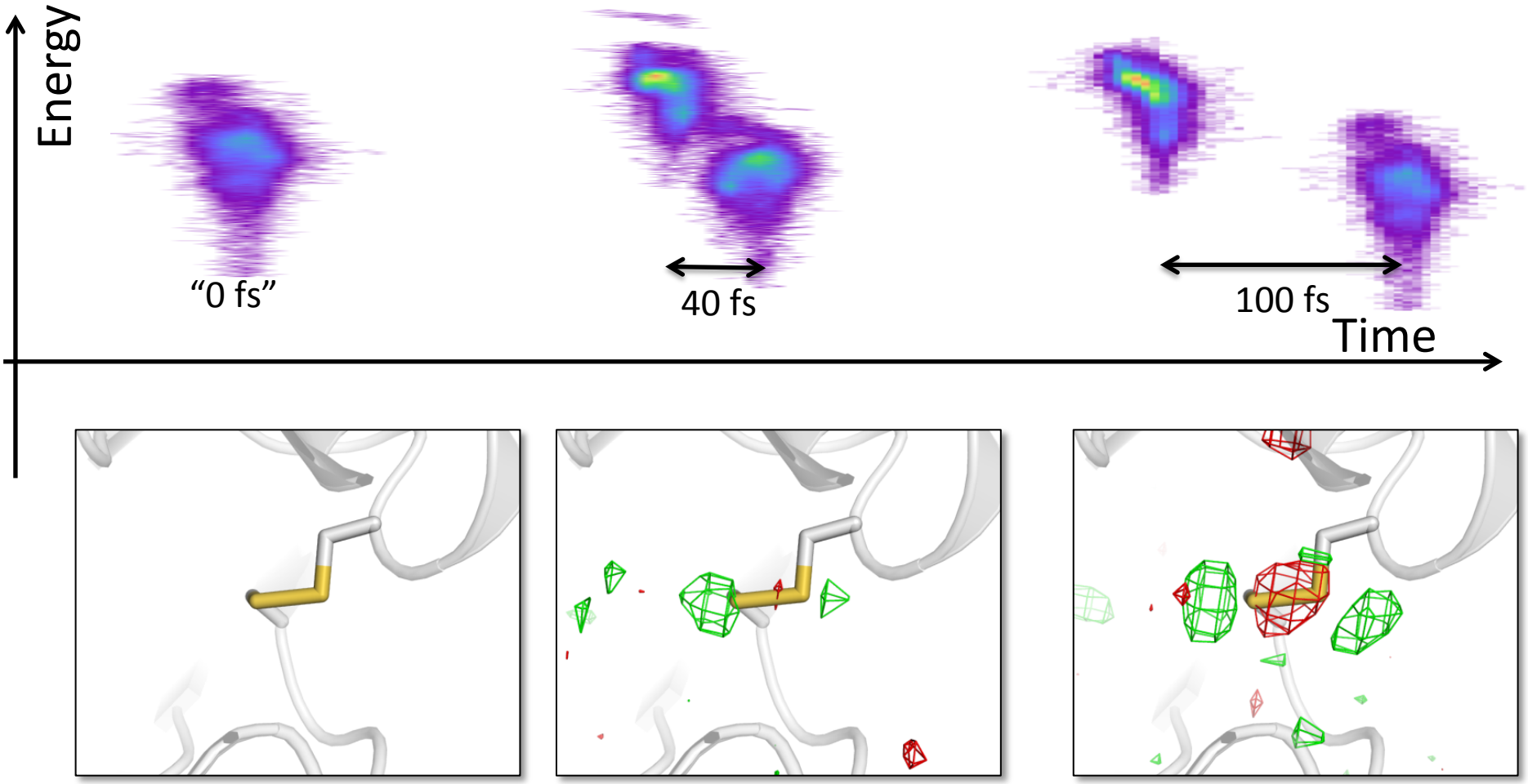

Pump-probe time delay

UCLA

Two-color pump-probe experiments with a twin pulse seed extreme ultraviolet free-electron laser, E. Allaria et al. Nature Comm., DOI: 10.1038/ncomms3476 (2013)

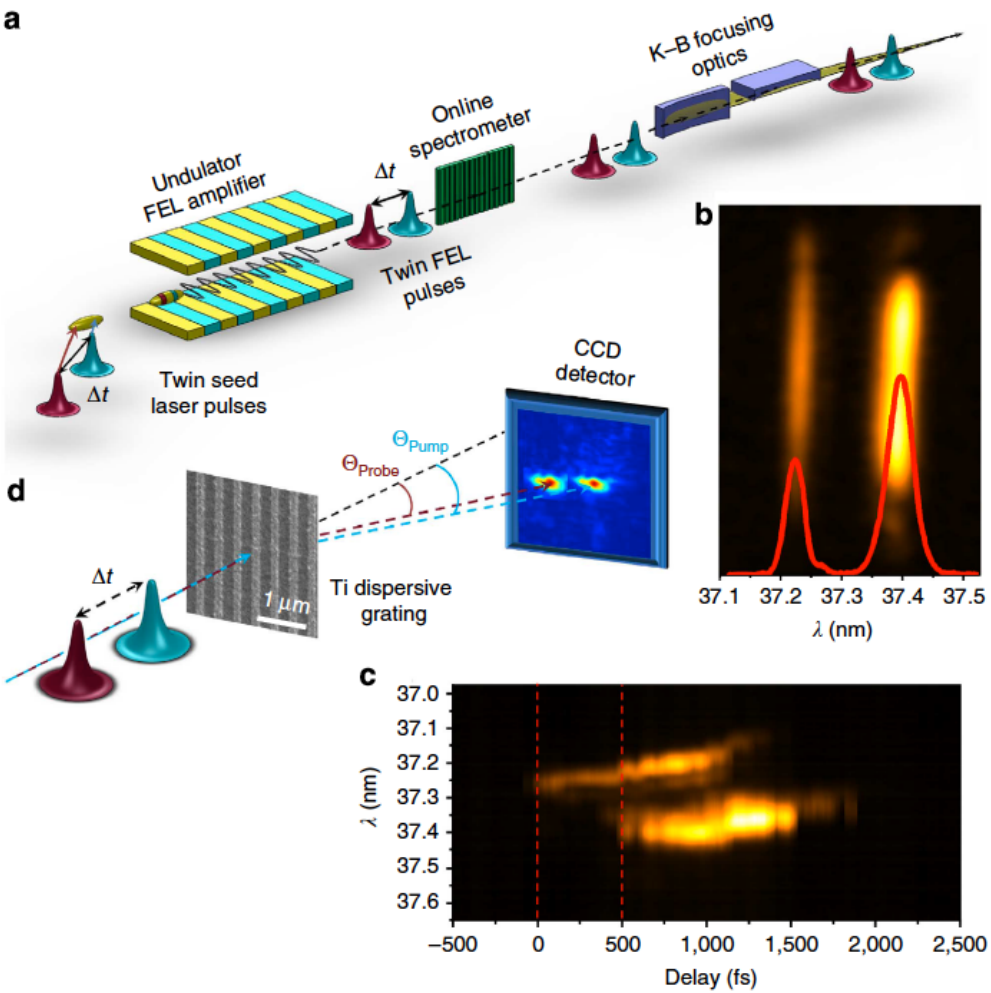

Fermi uses two different wavelength seed laser pulses, 180 fs long, seed at 260-262 lambda, fundamental at 784 nm, color separation inside gain bandwidth. The two pulses are separated in time and in wavelength.

PRL 111, 134801 (2013) PHYSICAL REVIEW LETTERS week ending 27 SEPTEMBER 2013

Multicolor Operation and Spectral Control in a Gain-Modulated X-Ray Free-Electron Laser

A. Marinelli,[1,*] A. A. Lutman,[1] J. Wu,[1] Y. Ding,[1] J. Krzywinski,[1] H.-D. Nuhn,[1] Y. Feng,[1] R. N. Coffee,[1] and C. Pellegrini[2,1]

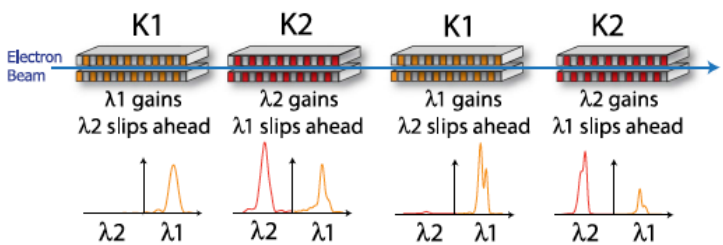

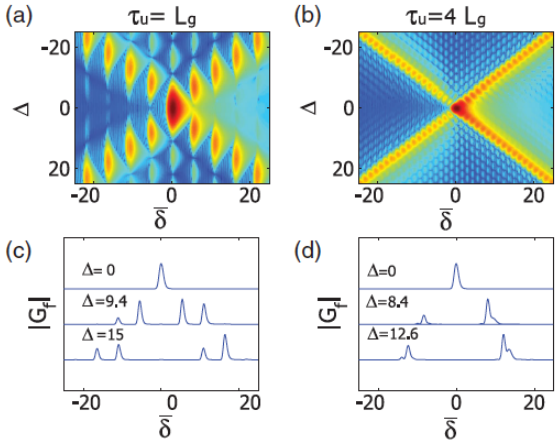

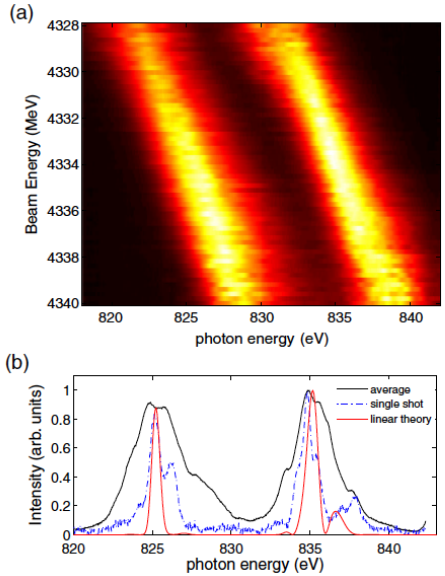

2 colors are simultaneous, important for stimulated emission. Line separation larger than bandwidth. Delay effect reduces bandwidth.

PRL **110,** 134801 (2013) PHYSICAL REVIEW LETTERS week ending 29 MARCH 2013

Experimental Demonstration of Femtosecond Two-Color X-Ray Free-Electron Lasers

A. A. Lutman, R. Coffee, Y. Ding,* Z. Huang, J. Krzywinski, T. Maxwell, M. Messerschmidt, and H.-D. Nuhn

Demonstration Of Two-color X-FEL Operation and Autocorrelation Measurement at SACLA, T.Hara, Y. Inubushi, T. Ishikawa, H. Tanaka, T. Tanaka, K. Togawa, M. Yabashi, T. Katayama, T. Togashi, K. Tono, T. Sato, Proc. of the 2013 FEL Conf. New York

PRL **111,** 134801 (2013) PHYSICAL REVIEW LETTERS week ending 27 SEPTEMBER 2013

Multicolor Operation and Spectral Control in a Gain-Modulated X-Ray Free-Electron Laser

A. Marinelli,[1,*] A. A. Lutman,[1] J. Wu,[1] Y. Ding,[1] J. Krzywinski,[1] H.-D. Nuhn,[1] Y. Feng,[1] R. N. Coffee,[1] and C. Pellegrini[2,1]

Exploring Vibration Modes in Gold Nanocrystals

UCLA

Ultrafast Three-Dimensional Imaging of Lattice Dynamics in Individual Gold Nanocrystals, J. N. Clark et al., Science, 341, 6141 (2013)

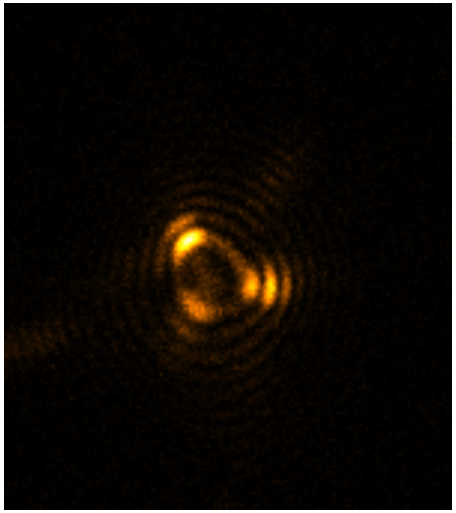

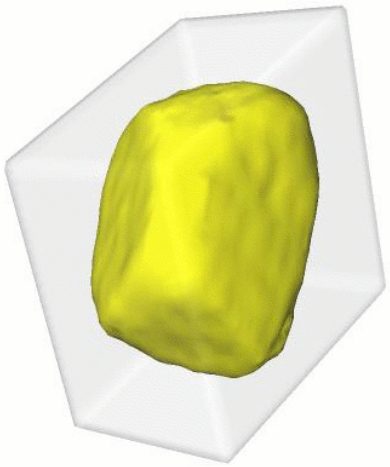

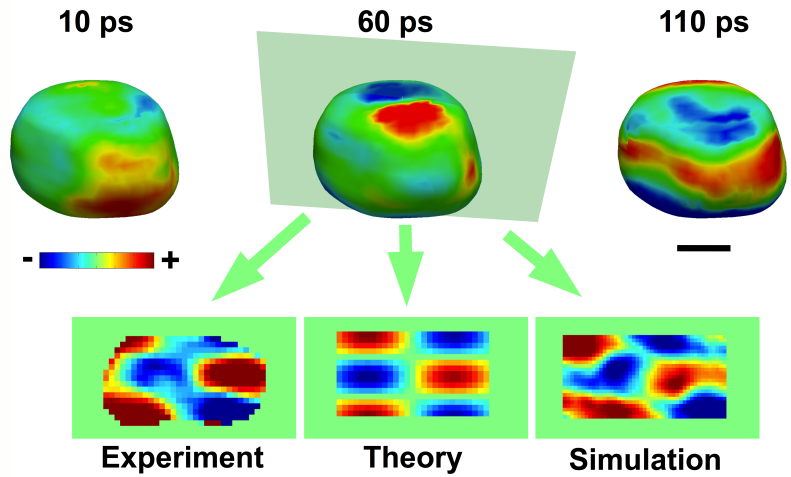

Key insights into the behavior of materials can be gained by observing their structure as they undergo lattice distortion.

Acoustic vibrations in gold nanocrystals (300-400 nm) triggered with infrared light pulses

- High-resolution real-space images of the deformation field inside the nanocrystal were obtained via the Bragg coherent diffraction imaging technique at various time delays
- Technique can extend to nanoscale objects of importance to catalysis and energy storage

Real Time Observation of Surface Bond Breaking in CO on Ru(0001) by Ultrafast Soft X-ray Spectroscopy

UCLA

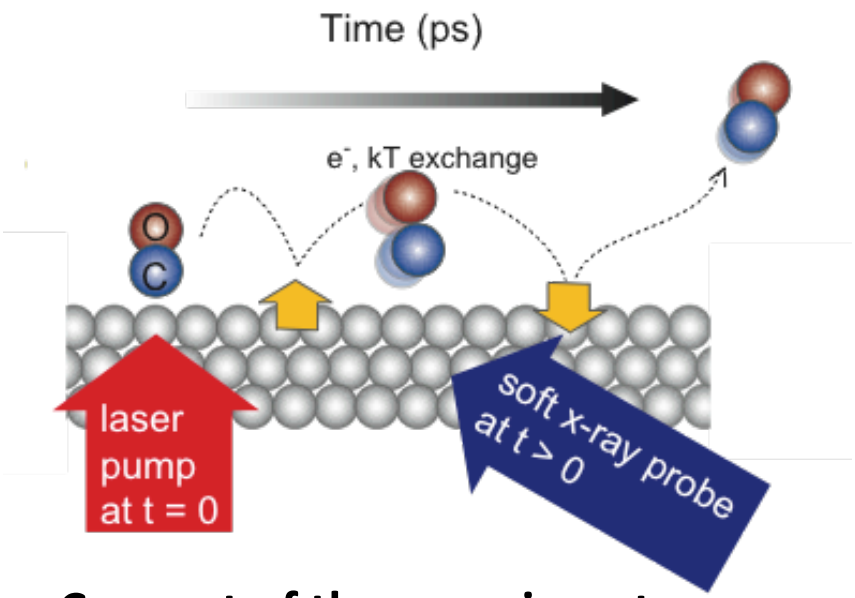

Concept of the experiment

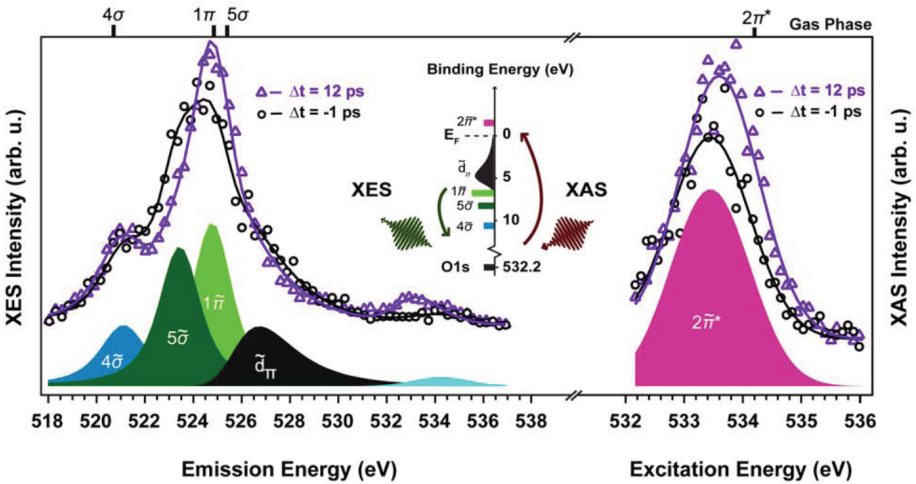

Oxygen K-edge XES (left) and XAS (right) spectra of CO/Ru(0001) measured at two selected pump-probe delays

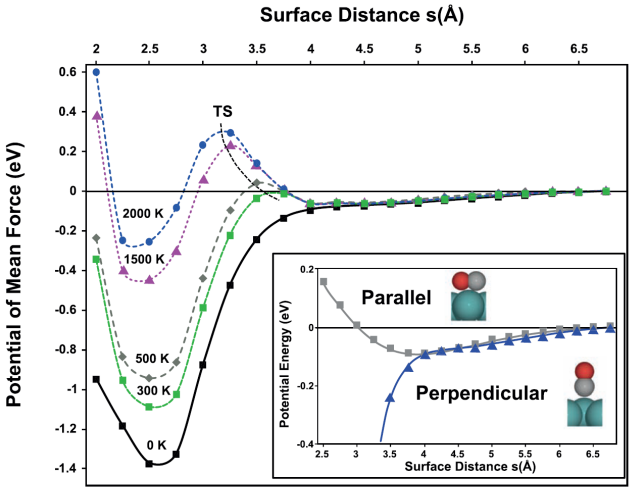

Dell'Angela et al, Science, 339, 6125 (2013)
Beye et al, Phys. Rev. Lett. 110, 18610 (2013)
Katayama et al. J. Electron Spectr. 187, 9. (2013)

UCLA

High Contrast X-ray Speckle from Atomic-Scale Order in Liquids and Glasses, S. O. Hruszkewycz et al., Phys. Rev. Lett. 109, 185502 (2012)

Ultrafast pulses of coherent hard x rays from the LCLS opens new opportunities for studies of atomic-scale dynamics in amorphous materials. The paper shows that single ultrafast coherent x-ray pulses can be used to observe the speckle contrast in the high-angle diffraction from liquid Ga and glassy Ni_2Pd_2P and B_2O_3. The experiment measures the thresholds for X-ray intensity to leave the atomic arrangement undisturbed. High contrast speckles are observed below this threshold, opening new opportunities for studies of atomic-scale dynamics in amorphous materials.

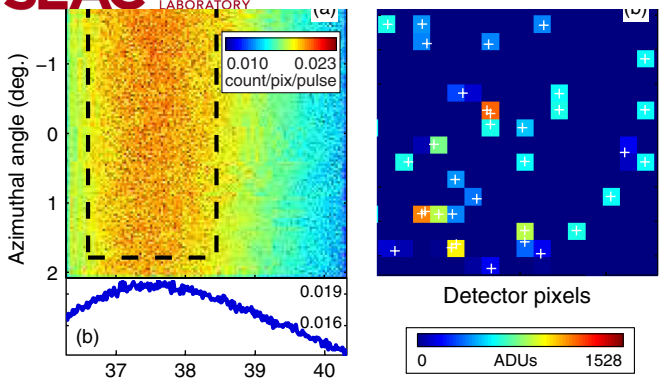

(a) Average scattering of liquid Ga integrated over 309 pulses from LCLS. Detector at 37 cm from the sample subtends scattering angles including the main amorphous scattering ring at Q= 2.60 $Å^{-1}$. Dashed box shows region of pixels used in contrast analysis. (b) Average photon density vs scattering angle. (c) Expansion of small region of a single-pulse scattering pattern showing signal in analog-to- digital units (ADUs) from individual photons, and assignment of photon positions.

- Experiments at LCLS X-ray Pump-Probe instrument, using a Si (111) monochromator with 1.4×10^{-4} bandwidth set to 7.99 keV photon energy, and 70 fs pulse width. Average x-ray pulse intensity between $(1\text{-}4)\times 10^{10}$ photons/ pulse.
- Important step to use coherent x-rays as powerful new probes of atomic scale structure and dynamics in non-crystalline systems, analogous to the techniques to study disorder at larger length scales using coherent visible light.
- The study of non-crystalline systems and non-equilibrium states is an important new area opened by X-ray FELs. These measurements are the first snapshots of the rapid atomic rearrangements that occur in a liquid.

SLAC NATIONAL ACCELERATOR LABORATORY

nature physics

ARTICLES

PUBLISHED ONLINE: 31 AUGUST 2015 | DOI: 10.1038/NPHYS3452

Anomalous nonlinear X-ray Compton scattering

Matthias Fuchs et al.

PUBLISHED ONLINE: 31 AUGUST 2015 | DOI: 10.1038/NPHYS3452

we report the observation of one of the most fundamental nonlinear X-ray–matter interactions: the concerted nonlinear Compton scattering of two identical hard X-ray photons producing a single higher-energy photon.

X-ray intensity reached 4×10^{20} W/cm^2, corresponding to an electric field, 5×10^{11} V/m, well above the atomic unit of strength and within almost four orders of magnitude of the quantum electrodynamics Schwinger critical field ~10^{18} V/m

Incoming photon energy ~9 keV, focus 100 nm, 1.5 mJ/pulse, 50 fs pulse duration.

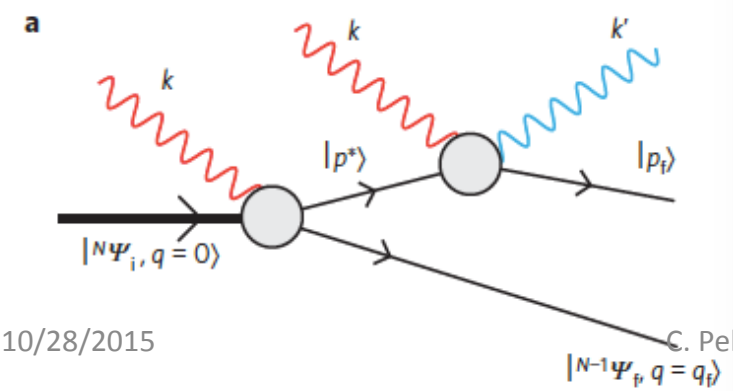

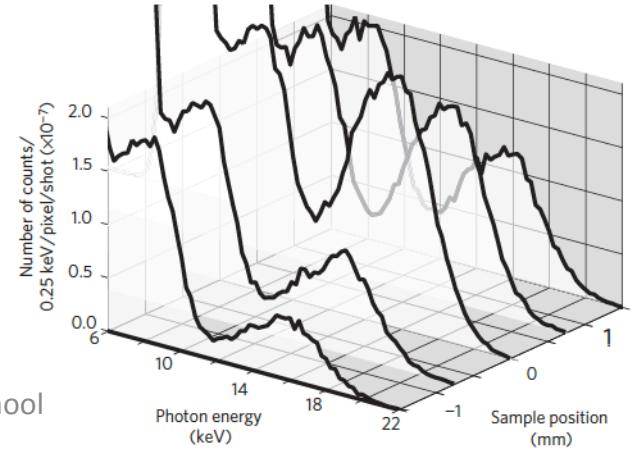

Matter in Extreme

Long pulse laser system

- Shock compression
- High pressure states

Short Pulse Laser	
Wavelength	800 nm
Pulse Width	35 fs
Repetition Rate	10 Hz
Pulse Energy	120 mJ

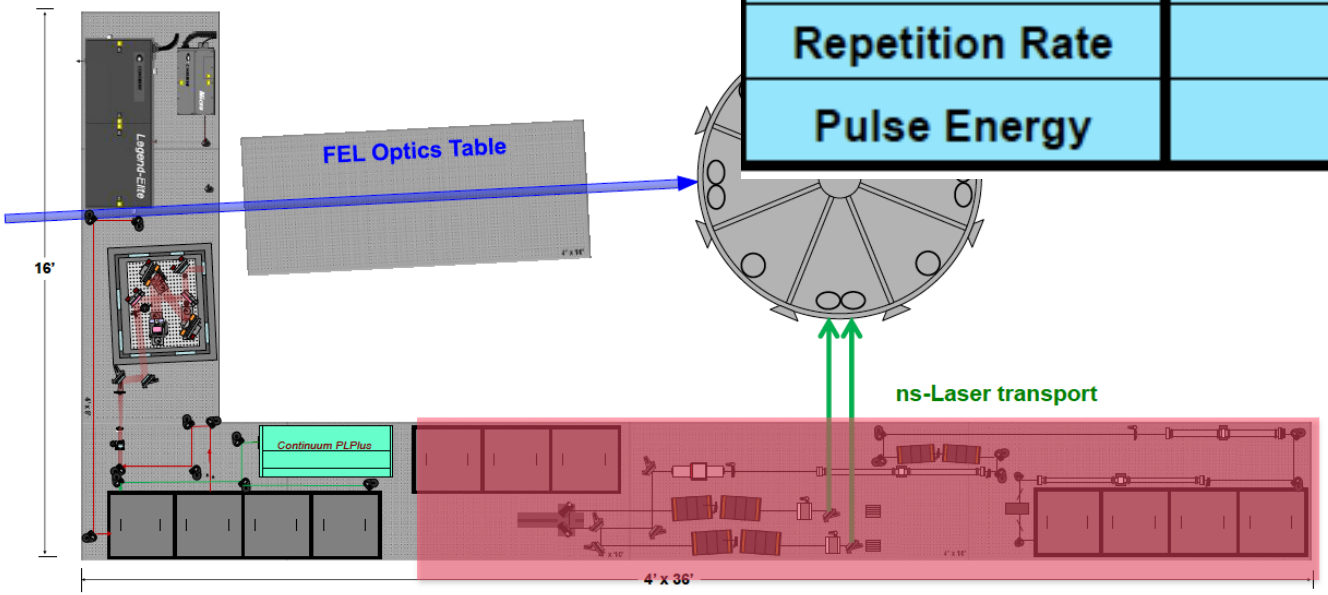

In operation from April 2012

Long Pulse Laser	
Wavelength	527 nm
Pulse Width	2-200 ns
Repetition Rate	1 shot per 10 minutes
Pulse Energy	2 x 15 Joules

Courtesy Siegfried Glenzer

PRL 109, 065002 (2012)
Selected for a Viewpoint in *Physics*
PHYSICAL REVIEW LETTERS
week ending
10 AUGUST 2012

Direct Measurements of the Ionization Potential Depression in a Dense Plasma

O. Ciricosta et al.

We have used the Linac Coherent Light Source to generate solid-density aluminum plasmas at temperatures of up to 180 eV. By varying the photon energy of the x rays that both create and probe the plasma, and observing the K-α fluorescence, we can directly measure the position of the K edge of the highly charged ions within the system. The results are found to disagree with the predictions of the extensively used Stewart-Pyatt model, but are consistent with the earlier model of Ecker and Kroll, which predicts significantly greater depression of the ionization potential.

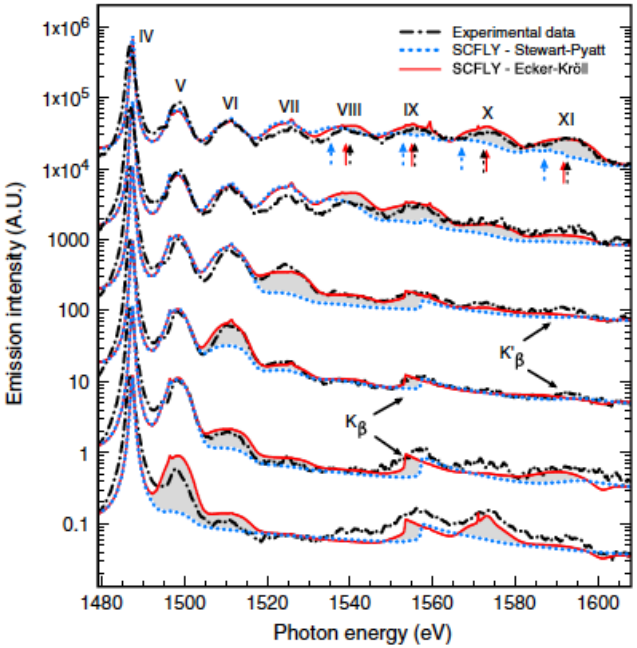

Recorded K-α emission spectra from hot solid-density aluminum. SCFLY simulations with different IPD models are compared with the experimental data for a subset of the x-ray laser photon energies. From the bottom, the spectra corresponding to 1580, 1600, 1630, 1650, 1720 and 1830 eV pump photon energies are shown. The spectra have been artificially displaced in intensity for clarity, and a bremsstrahlung component (at the maximum temperature provided by the simulations) has been added to the calculated spectra. The grey shading indicates the difference between the calculations using different IPD models.

Diffraction before destruction

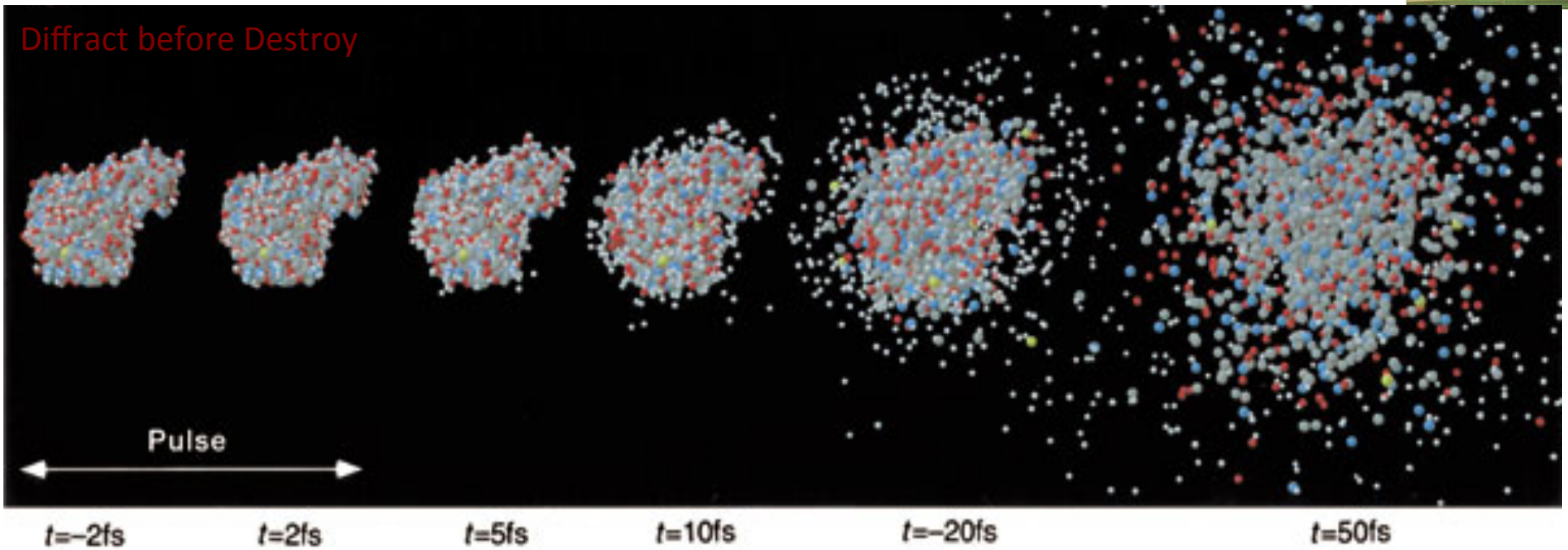

Neutze, R.,Wouts, R., van der Spoel, D.,Weckert, E. & Hajdu, J. Potential for biomolecular imaging with femtosecond X-ray pulses. Nature 406, 752–757 (2000).

Incoherent vs. coherent X-ray beams

UCLA

PAST:

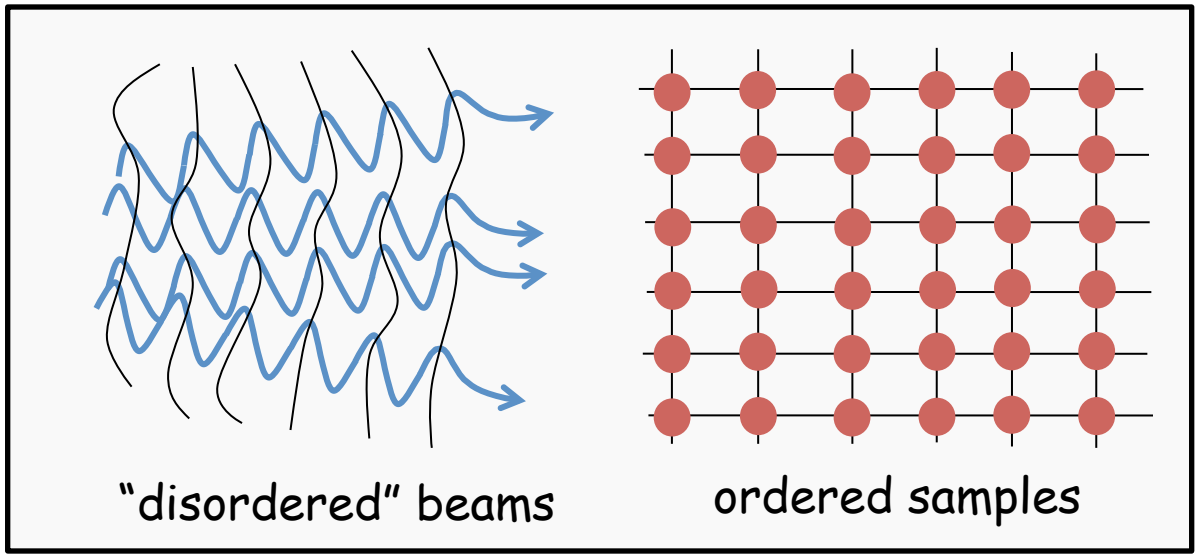

FUTURE:

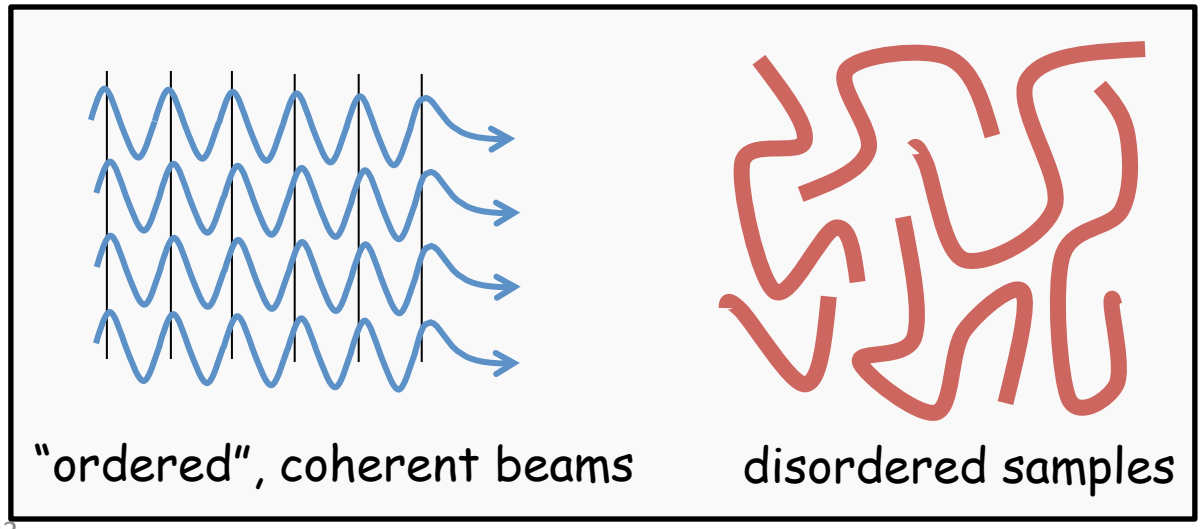

X-ray Crystallography

UCLA

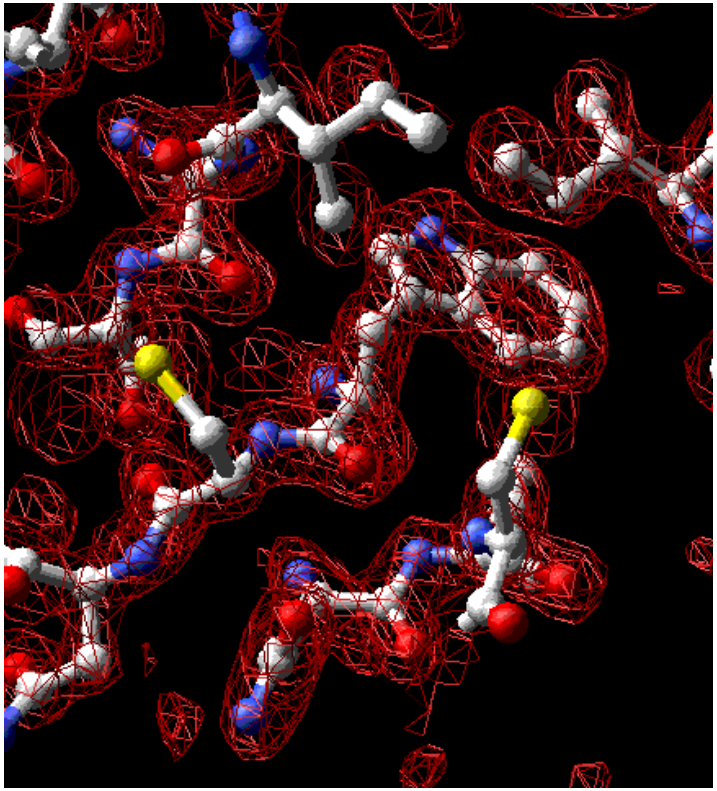

$$F(\mathbf{q}) = F_c(\mathbf{q}) \prod_{j=1}^{3} \frac{\sin(N_j \mathbf{q}\cdot\mathbf{a}_j/2)}{\sin(\mathbf{q}\cdot\mathbf{a}_j/2)}$$

80% of the structures in PDB Data Bank were determined by using x-ray crystallography.

In X-ray crystallography, protein first needs to be purified and crystallized, which may take months or years to complete, if not failed.

'The phase problem' is the problem of determining the phases when only the magnitudes are known.

A structural biology example of X-ray FELs impact:

510 Biophysical Journal Volume 106 February 2014 510–525

Biophysical Highlights from 54 Years of Macromolecular Crystallography

Jane S. Richardson* and David C. Richardson
Biochemistry Department, Duke University, Durham, North Carolina

ABSTRACT The United Nations has declared 2014 the International Year of Crystallography, and in commemoration, this review features a selection of 54 notable macromolecular crystal structures that have illuminated the field of biophysics in the 54 years since the first excitement of the myoglobin and hemoglobin structures in 1960. Chronological by publication of the earliest solved structure, each illustrated entry briefly describes key concepts or methods new at the time and key later work leveraged by knowledge of the three-dimensional atomic structure.

54. Free-electron laser crystallography

Free-electron laser crystallography is without question the most spectacular new technical development in the field. A jet of droplets with nanocrystals is sent past a beam of femtosecond x-ray laser pulses, and diffraction is recorded before the crystal has time to explode. This has the potential for determining otherwise intractable molecular structures and for accessing rapid time steps. The many challenging problems with data and analysis appear to be solvable. After demonstration structures of photosystems and lysozyme (e.g., PDB:3PCQ (126), PDB:4FBY (127), PDB:4ET8 (10)), there is now a novel structure of propeptide-inhibited trypanosomal cathepsin B (PDB:4HWY (128)) potentially useful for drug design. (Fig. 54. Cα splines and chromophores (*pink*) in Photosystem II (PDB:4FBY)).

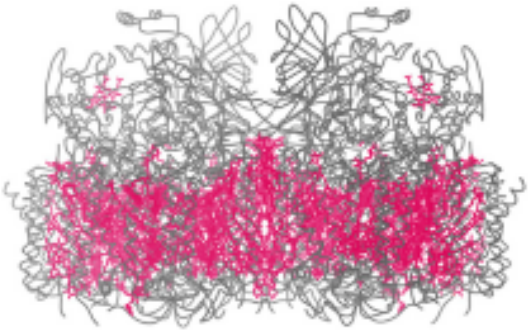

High-Resolution Protein Structure Determination by Serial Femtosecond Crystallography

Sébastien Boutet et al., *Science* **337**, 362 (2012)

UCLA

The experiments applies serial femtosecond crystallography (SFX) using an x-ray free-electron laser to obtain high-resolution structural information from microcrystals (less than 1 micrometer by 1 micrometer by 3 micrometers) of the well-characterized model protein lysozyme. The agreement with synchrotron data demonstrates the immediate relevance of SFX for analyzing the structure of the large group of difficult-to-crystallize molecules.

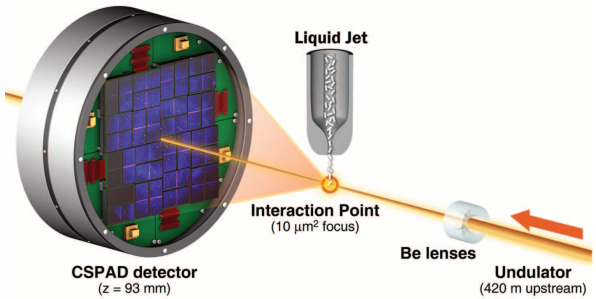

Experiment for SFX at the CXI instrument. Single-pulse diffraction patterns from single crystals flowing in a liquid jet are recorded on a CSPAD at 120-Hz. Each pulse is focused at the interaction point by using 9.4-keV x-rays. The sample-to-detector distance (z) is 93 mm. 1.5 million individual “snap- shot” diffraction patterns, 40-fs pulses, at LCLS repetition rate of 120 Hz. 4.5% of the patterns classified as crystal hits, 18.4% of which indexed and integrated with the CrystFEL software showing excellent statistics to 1.9 Å resolution

UCLA

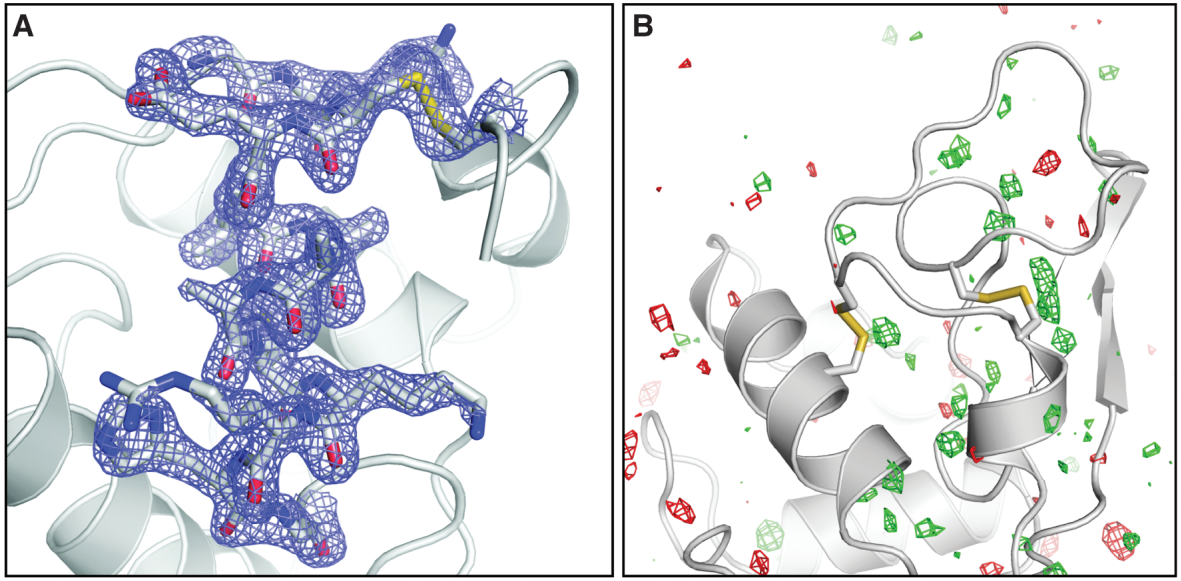

A) Final, refined 2mFobs – DFcalc (1.5s) electron density map of lysozyme at **1.9 Å resolution** calculated from 40-fs pulse data. (B) Fobs(40 fs) – Fobs (synchrotron) difference Fourier map, contoured at +3 s (green) and –3 s (red). No interpretable features are apparent. The synchrotron data set was collected with a radiation dose of 24 kGy.

Natively Inhibited Trypanosoma brucei Cathepsin B Structure Determined by Using an X-ray Laser, L. Redecke et al. Science 339, 227 (2013)

UCLA

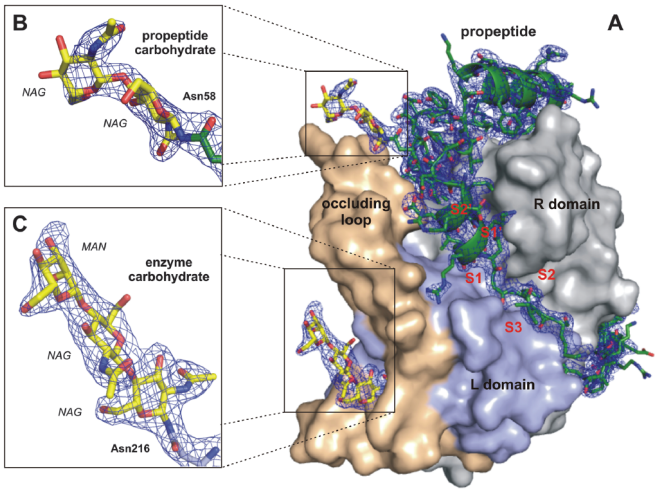

The Trypanosoma brucei cysteine protease cathepsin B (TbCatB), which is involved in host protein degradation, is a **promising target to develop new treatments against sleeping sickness, a fatal disease caused by this protozoan parasite.** …

By combining two recent innovations, in vivo crystallization and serial femtosecond crystallography, we obtained the room-temperature 2.1 angstrom resolution structure of the fully glycosylated precursor complex of TbCatB. The structure reveals the mechanism of native TbCatB inhibition and demonstrates that new biomolecular information can be obtained by the **"diffraction-before-destruction"** approach of x-ray free-electron lasers from hundreds of thousands of individual microcrystals.

Conclusions: 390 years of exploration of the microscopic world

Resolution: ~0.1 mm, 0.1 sec

F. Stelluti, 1625

Galileian microscope

Resolution: ~0.01 mm, 0.1 sec

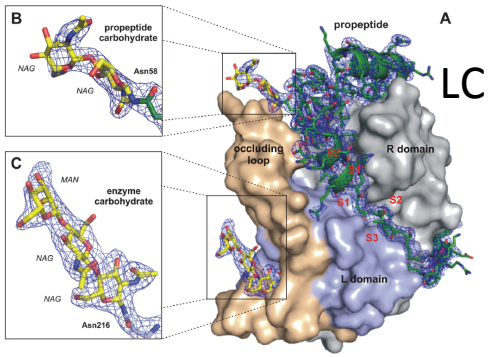

LCLS, 2009

Radecke et al, *Science* 339, 6116 (2012)

Resolution: ~few Å, few fs

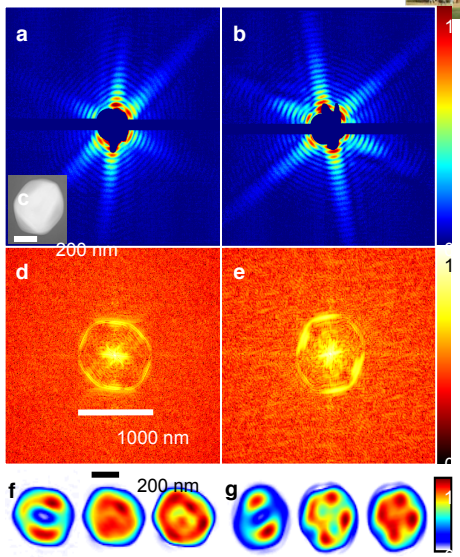

Seibert et al, *Nature*, 470, 78 (2011)

UCLA

Science and scientific instruments

Look! Up in the sky! It's a bird! It's a plane!

It's a scientist

Powers:
super strength, flight, invulnerability, super speed, heat vision, freeze breath, x-ray vision, superhuman hearing, healing factor